CHAPTER 6

Ionomeric Polymer-Metal Composites

Sia Nemat-Nasser and Chris W. Thomas
University of California, San Diego

6.1 Introduction

Ionomeric polymer-metal composites (IPMCs) as bending actuators and sensors are sometimes referred to as "soft actuators-sensors" or "artificial muscles." A typical IPMC consists of a thin (200 μm) polymer membrane with metal electrodes (5–10-μm thick) plated on both faces; see Fig. 1. The polyelectrolyte matrix is neutralized with an amount of counter-ions, balancing the charge of anions covalently fixed to the membrane. When an IPMC in the solvated (i.e., hydrated) state is stimulated with a suddenly applied small (1–3 V, depending on the solvent) step-potential, both the fixed anions and mobile counter-ions are subjected to an electric field, with the counter-ions being able to diffuse toward one of the electrodes. As a result, the composite undergoes an initial fast bending deformation, followed by a slow relaxation, either in the same or in the opposite direction, depending on the composition of the backbone ionomers and the nature of the counter-ion. The magnitude and speed of the initial fast deflection also depend on the same factors, as well as on the structure of the electrodes, and other conditions (e.g., the time-variation of the imposed voltage). IPMCs that are made from Nafion and are neutralized with alkali metals or with alkyl-ammonium cations (except for tetrabutylammonium,TBA^+), invariably first bend towards the anode under a step direct current (dc), and then relax towards the cathode, while the applied voltage is being maintained, often moving beyond their starting position. In this case, the motion towards the anode can be eliminated by slowly increasing the applied potential at a suitable rate. For Flemion-based IPMCs, on the other hand, the initial fast bending and the subsequent relaxation are both towards the anode, for all counter-ions that have been considered. With TBA^+ as the counter-ion, no noticeable relaxation towards the cathode has been recorded for either Nafion- or Flemion-based IPMCs. When an IPMC membrane is suddenly bent, a small voltage of the order of millivolts is produced across its faces. Hence, IPMCs of this kind can serve as soft actuators and sensors.

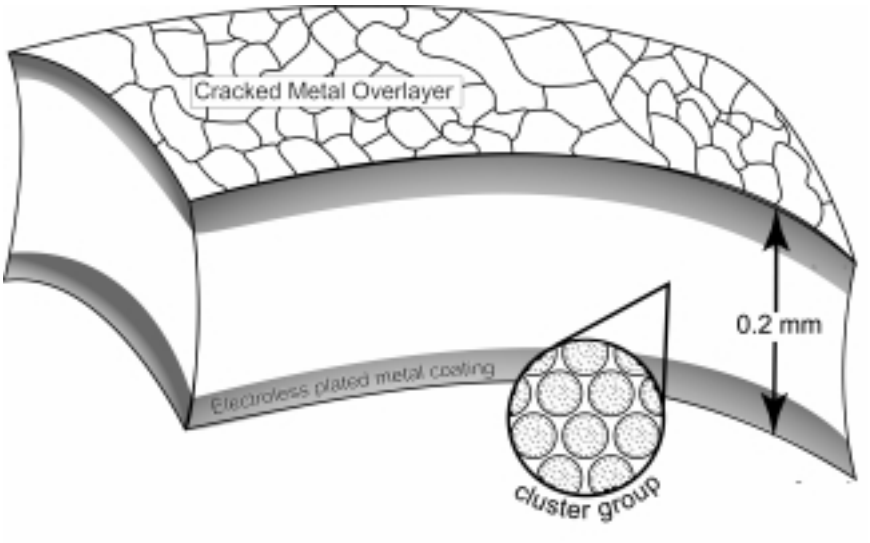

Figure 1: IPMC schematics indicating surface morphology, interface, and cluster structure.

In certain applications, IPMC materials may offer advantages over conventional mechanical, hydraulic, or pneumatic actuators, in that IPMCs lack moving parts and require only modest operating voltages for actuation. Investigations into the mechanism of IPMC actuation and sensing seek to foster development of actuators that generate greater displacement magnitudes and forces, and sensors that are more sensitive to imposed deformations. Developers seek to exploit these materials in a number of applications including medical, space, robotic, soft microelectronic machine (MEMS), and entertainment devices. This chapter addresses the known properties of IPMC materials, their manufacture, and the methods for their characterization. In addition, we provide a summary of models proposed to account for the mechanisms of IPMC actuation and sensing, experimental results to support or invalidate these models, and concluding with a hybrid model that integrates electrical, chemical, and mechanical forces to produce results in accord with experimental observations. Finally, we highlight a few applications that have been proposed for these materials.

6.2 Brief History of IPMC Materials

IPMCs represent one class of electroactive polymeric materials, a recent entry into a field of shape-modifying polymers that dates back more than 50 years. While a total survey of these materials is beyond the scope of this chapter, they have been addressed elsewhere [Segalman et al., 1992; Shahinpoor et al., 1998]. Recent developments in electroactive polymers are addressed throughout this

book, and it is the intention of this chapter to highlight the elements that distinguish IPMC materials from other electroactive polymers. One of the most significant aspects of IPMCs is their actuation based on the active (anisotropic, directional) motion of ions and solvent molecules within the membrane under applied stimulus, and other materials whose actuation derives from the passive (isotropic, volumetric) response to stimuli.

Polymer-metal composites were developed as early as 1939 via the precipitation of colloidal silver on prepared substrates [*Modern Plastics*, 1938; Feynman, 1985]. These early materials suffered from delamination of the metal overlayer, and were little more than decorative curiosities. Recently, sputtering methods have provided routes to polymer-metal composites, but these were prone to delamination as well [Bergman, 1970; McCallum and Pletcher, 1975]. Indeed, it was not until the late 1960s when researchers at Dow Chemical showed that the permselective properties of ionomeric resins could be used to facilitate selective reduction of metal salts at the surface of an ion exchange membrane using chemical reductants such as sodium borohydride ($NaBH_4$) or hydrazine (N_2H_4) [Levine and Prevost, 1968; Bartrum, 1969; Wiechen, 1971]. Later, these methods were applied to Nafion-type membranes by many Japanese groups, including workers at Hitachi [Hitachi, 1983; Sakai et al., 1985a; 1985b; Takenaka et al., 1982, 1985] in the early 1980s. Millet and coworkers further developed the technique of IPMC formation, characterizing the plating mechanism to improve the morphology of the metal electrodes in IPMCs [Millet et al., 1989, 1990, 1992, 1993, 1995]. Figure 2 displays the chemical structure of three perfluorinated ionomers used to produce IPMCs, varying in the length and number of side chains and in the nature of ionic side group—usually sulfonate or carboxylate anions. As will be discussed, the acidity strength of the ionic side group has a profound effect on the actuation of the resulting IPMC [Nemat-Nasser and Wu, 2003a], and, indeed, lies at the root of the back-relaxation mechanism in Nafion-based IPMCs.

IPMC materials were developed as solid polymer electrolyte fuel cell membranes [Kordesch and Simader, 1995]. During investigations into the use of IPMCs as hydrogen pressure transducers, Sadeghipour et al. [1992] found that IPMC materials could act as vibration sensors. They reported that a platinum-IPMC in the Na^+ form generated over 12 mV/g of acceleration. The maximum volt response of their sensor occurred at 2000 Hz oscillation. These authors point out that the dynamic behavior of their "cell" filters and amplifies vibratory input to the IPMC, and that the signal response of the IPMC is not strongly frequency

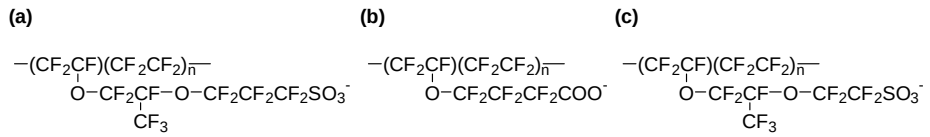

Figure 2: Perfluorinated ionomers used in IPMC manufacture include (a) Aciplex, (b) Flemion, and (c) Nafion.

dependent. In noting that the transduction of an IPMC generates a voltage, Sadeghipour and coworkers should be credited for proposing this material as a soft sensor. It should be noted that they were tantalizingly close to discovering IPMC's use as an actuator. Instead, in Japan, that same year, Oguro et al. described the ability of an IPMC material to bend under an applied voltage [1992]. In the USA, researchers, such as Mojarrad and Shahinpoor [1996], have since sought to improve the performance of Nafion-based IPMC actuators through optimization of the method of manufacture, including sample size, dimensions, and particularly the electrode morphology. More recently, Nemat-Nasser [2002], Nemat-Nasser and Wu [2003a], and Nemat-Nasser and Zamani [2003] have performed thorough and systematic studies of the properties and actuation of both Nafion- and Flemion-based IPMCs, in various cation forms and with different solvents, seeking to identify the underpinning mechanisms of actuations, model the phenomena of the IPMC actuation and sensing in order to predict properties quantitatively and relate these to the composition, processing, and microstructure of IPMC materials.

6.3 Materials and Manufacture

6.3.1 Ionomer (Nafion) Structure

For convenience, to date all IPMC materials known to us have used commercially available perfluorinated ionomeric polymer membranes. Several vendors offer ionomer membranes, including DuPont (Nafion), Asahi Glass (Flemion), Asahi Chemical (Aciplex), and others. The general method [Millet, 1999] for preparing IPMCs consists of three basic steps, as shown in Fig. 3. After cleaning with strong acids such as HNO_3, a clean sample of the

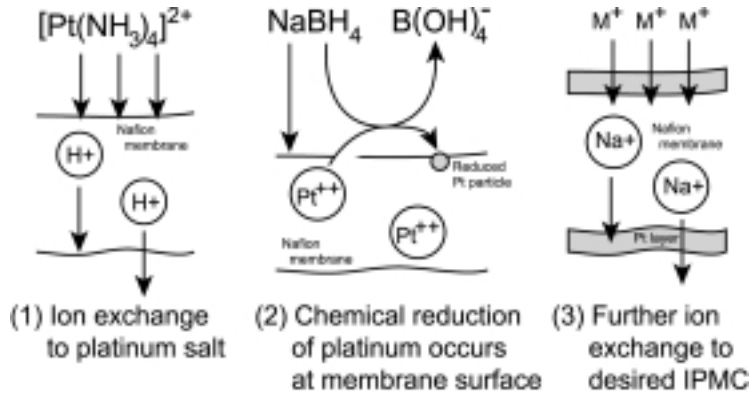

Figure 3: Scheme for IPMC fabrication: (1) ion exchange with noble metal salt; (2) reduction of metal at surface; (3) ion exchange with desired cation.

*poly*perfluoroethylenesulfonate membrane is soaked in a solution of an appropriate metal salt [e.g., $Pt(NH_3)_4Cl_2$] to populate each ionomer exchange site with reducible metal. The prepared sample is immersed in a solution of a suitable chemical reductant, such as sodium borohydride, which cannot penetrate into the ion exchange membrane. The metal salt diffuses out of the membrane and is reduced when it encounters the reducing agent at the surface of the membrane. The reduction process creates metal particles between 3 and 10 nm in diameter. The distribution of the metal plate is greatest at the surface of the membrane, and decreases significantly through the first 10–20-μm depth into the membrane (Fig. 4), although some particles are found throughout the membrane sample, even at its center. Optimizations of the techniques for IPMC manufacture have been reported by Liu et al. [1992], Homma and Nakano [1999], and Rashid and Shahinpoor [1999].

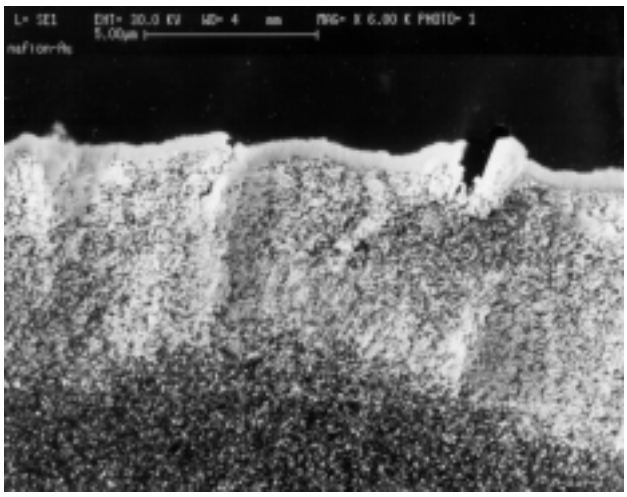

Figure 4: Transmission electron micrograph (TEM) of Pt/Au-IPMC. A cross section at the surface indicates a gold overcoating and the decay in metal (Pt) concentration deeper within the Nafion ionomer.

Variations of IPMC manufacture have been reported: Fujita and Muto describe a method in which platinum is precipitated in the presence of a solution of Nafion125, and the resulting mixture of Nafion and colloidal platinum is then coated onto the surface of a Nafion membrane [Fujita and Muto, 1986]. IPMC materials have been made using a number of different metals including Ni, Pb, Cu, Ag [Chen and Chou, 1993], Au [Oguro et al., 1999; Fujiwara et al., 2000] and Ir [Millet et al., 1989]. Formation of cadmium selenide (CdS) clusters within Nafion membranes has been reported [Nandakumar et al., 1999]. Metal reduction has been accomplished using gamma radiation, as reported by Platzer et al. [1989], and Belloni et al. [1998]. As well, Salehpoor et al. [1998] have prepared IPMCs by chemical vapor deposition. For IPMCs manufactured from anion

exchange membranes, see Dube [1998]. Si et al. [1998] have reported on possible mechanisms for platinum particle synthesis, and have noted preferential growth of Pt(111) crystal faces in IPMC materials. Bennett and Leo [2003] have manufactured and characterized IPMCs with non-precious metal electrodes.

Optical micrographs and SEM images of the surfaces of plated IPMCs indicate a two-part construction of these materials. Beyond the surface of the membrane, a thicker overlayer of metal is deposited, usually less than 10-μm thick. Optimization of this layer is crucial, as greater thicknesses yield greater surface conductivity—essential in charging the membrane and generating actuative bending. At the same time, greater metal thicknesses increase the composite's stiffness, increasing the force required for the same displacement.

In a recent work, Nemat-Nasser and Wu [2003a] have examined the microstructure and actuation of Flemion-based IPMCs, having gold electrodes of fine dendritic structure, comparing the response of this composite with that of Nafion-based IPMCs in various cation forms. Figure 5 shows the electrode morphology of a Flemion-based IPMC.

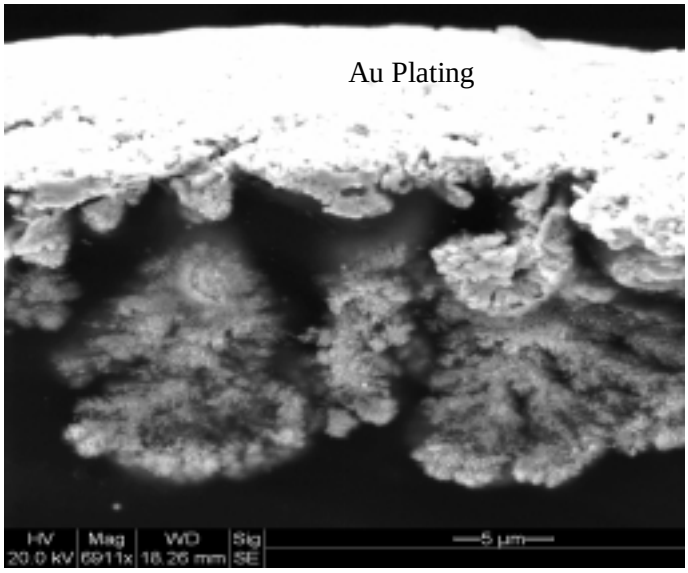

Figure 5: Cross section of a typical Au-plated Flemion-1.44, showing dendritic structure of gold electrodes.

The metal surface in an IPMC usually appears fractured, displaying discrete islands of metal deposition between 5–20 μm across, as shown in Fig. 6. It is presumed that water swelling and electroactive bending generate these islands when the resulting strains exceed the tensile strength of the thin metal layer. This process is not well studied, and anecdotal evidence suggests that IPMC actuators

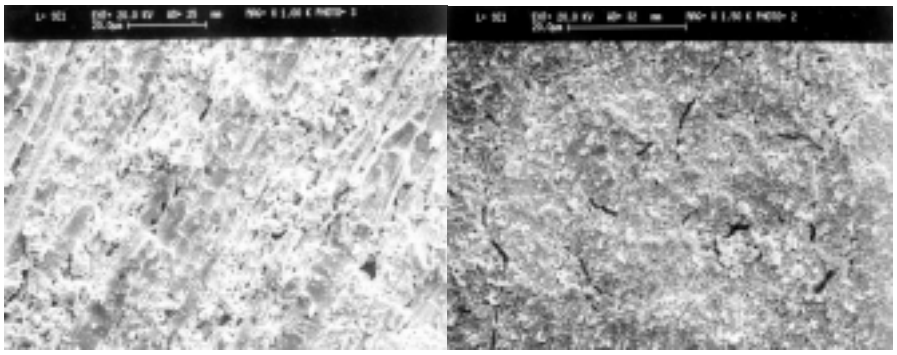

Figure 6: Scanning electron microscopic photos of IPMC surfaces, showing microcracks on Nafion- (left) and on Flemion- (right) based IPMCs.

require an initial "working" of the sample to develop sufficient surface fractionation. Regardless of the presence of fractionation, surface conductivity must be sufficiently large to produce maximum actuation, as conduction occurs through the metallic underlayer or via contact of individual metal islands at the surface of the membrane.

6.4 Properties and Characterization

As stated before, if an IPMC sample in the solvated (i.e., hydrated) state is suddenly bent, a voltage is produced across its faces. If, on the other hand, the same strip has an alternating voltage imposed across its faces, the sample exhibits an oscillatory bending motion. When the same strip is subjected to a suddenly imposed and sustained constant voltage (dc) across its faces, the initial relatively "fast" displacement is generally followed by a slower relaxation, in the reverse direction for Nafion-based IPMCs and in the same direction for Flemion-based IPMCs, in aqueous or other environments. Finally, when the two faces of the strip are shorted during this slow relaxation, a sudden fast motion, in the same direction for Nafion-based and in the opposite direction for Flemion-based IPMCs, occurs. This is then followed by slow relaxation in the opposite (Nafion-based) or the same (Flemion-based) direction. By imposing a ramp voltage of a suitable constant rate, the initial motion towards the anode can be eliminated for Nafion-based IPMCs in all tested cation forms (except for TBA^+). Improvements in the sensing and actuating attributes of IPMC materials have involved measurement of the actuation and sensing properties of the material, as well as modeling to understand the underpinning actuation and sensing mechanisms.

The first improvements in IPMCs' bending response were obtained by optimizing the method of IPMC fabrication. Building on the work of Millet et al., Shahinpoor and coworkers developed a number of improved forms by varying the metal ion used, the chemistry of metal reduction, and the surface treatments of IPMC samples [Rashid and Shahinpoor, 1999]. On a different tack, Oguro et al. [1992] drew from the work of Takenaka et al. [1982] and researchers at

Hitachi [Hitachi Patent, 1983], adopting a method that includes the use of hydrazine during chemical reduction.

A second round of investigation indicated the strong influence of countercation species on the actuation and sensing behavior of IPMCs [Abé et al., 1998]. These studies were limited to monovalent cations such as alkali metal salts or tetraalkylammonium salts. Some early results from these investigations showed that lithium salts produced the greatest displacement of the tip of a cantilever strip over other alkali metals; this may be due to the effect of the countercation on the bending stiffness of the strip, on the resulting internal forces, or on both, as is discussed in Sec. 6.4.7. Other alkali metals showed different degrees of tip displacement and large variation in the extent of slow reverse relaxation. Tetrabutylammonium (TBA^+) samples exhibit the interesting property that dc actuation produces a slow deformation and no observed back relaxation in either Nafion- or Flemion-based IPMCs. On the other hand, lithium-containing Nafion-based samples have been observed to exhibit fast actuation followed by some small reverse relaxation [Nemat-Nasser and Li, 2000; Nemat-Nasser, 2002], while extensive back relaxation is observed for sodium-, potassium, rubidium-, cesium-, thallium-containing Nafion-based IPMCs [Nemat-Nasser and Thomas, 2001; Nemat-Nasser and Wu, 2003a; Nemat-Nasser and Zamani, 2003]. Combined Na^+ and TBA^+ cations have been used to tailor the actuation of Nafion-based IPMCs, thereby controlling the initial speed of bending towards the anode and the subsequent relaxation in the opposite direction [Nemat-Nasser and Wu, 2003b].

Throughout our investigations, focus has been placed on understanding the mechanisms of actuation and sensing, in order to understand these materials and improve their performance. We accomplish this by examining the effect of the nature of the backbone ionomer, the morphology of the metal electrode, the countercation, or the solvent used to produce the IPMC, as well as the optimization of the procedures of electrode deposition and sample preparation.

6.4.1 Polymer Properties

Nafion is a perfluorinated copolymer of polytetrafluoroethylene (PTFE) and a perfluorinated vinyl ether sulfonate. Varying the nature of the vinyl ether side chain gives routes to alternative species, usually through the addition of single CF_2 groups (Aciplex) or modification of the length of the side chain (Flemion). Within a limited range, the ratio of monomers can be used to tailor the polymer equivalent weight (grams dry polymer per mole of ion), although large variation can significantly influence the strength, flexibility, and stability of the resulting membranes. Primary physical data for fluorinated ionomers have been summarized [Fernandez, 1999].

Small-angle x-ray scattering [Roche et al., 1981] and TEM analysis [Xue et al.1989] of Nafion (hydrated and dry H^+ and Na^+ membranes) indicate an essentially constant spacing at about 50 Å with an intensity dependent on water content. This spacing has been attributed to the spacing between individual ionic

cluster domains within the Nafion structure [Gierke et al., 1981]. These domains are a result of the particular structure of Nafion polymers. Presumably, the hydrophobic PTFE backbones aggregate to form a semicrystalline matrix and the individual side chains orient their hydrophilic-end groups to form water-filled clusters [Heitner-Wirguin, 1996]. James et al. [2000] have used atomic force microscopy (AFM) to probe the surface of Nafion membranes under a variety of hydration conditions. They observe small clusters (2–5-nm diameter) gathering into super-clusters up to 30-nm diameter. Upon hydration, they noted that the total number of clusters decreases while the size of each cluster increases, suggesting a cluster-consolidation model for Nafion hydration.

6.4.2 Ion-Exchange Capacity

The ion-exchange capacity of an IPMC material indicates the number of sulfonate (Nafion) or carboxylate (Flemion) groups within a fixed volume of material. This number should correspond to the number of substituted (non-H^+) charge-balancing cations within the IPMC. During preparation, sheets of bare Nafion are surface roughened by sanding or sandblasting. Ablation of the ionomeric polymer reduces the mass of the ionomer and, thus, the total moles of ion per cm^2 of sheet. (Note that the measurement of IPMCs in cm^2 derives from the fact that these materials are prepared and handled in sheet form.) Moreover, the addition of metal to the membrane increases the density of the IPMC. Since a sample of IPMC weighs more than bare Nafion and contains fewer ionic sites per unit mass, the equivalent weights of plated samples is larger than the bare Nafion. The required scaling factor can be found by dissolving the metal over layer in aqua regia and determining the mass of remaining IPMC. We find for some early IPMC samples provided to us by Shahinpoor [Shahinpoor, M., personal communication; Rashid and Shahinpoor, 1999] that they are composed of Nafion117, approximately 88% by volume (58% by weight). More recently, similar results (about 59 to 61% by weight) were reported by Nemat-Nasser and Wu [2003a] for various samples that have been plated by Shahinpoor and coworkers.

Because of these modifications to the sample composition during plating, a sample's equivalent weight changes. Equivalent weight is an operational quantity, representing the mass of dry IPMC that contains one mole of ion. For IPMCs containing ions other than protons, the true equivalent weight is given by

$$EW_{\text{Ion}} = \frac{EW_{H+} - 1.008 + FW_{\text{Ion}}}{SF},$$

where EW_{H+} is the equivalent weight of the dry ionomer in proton form (1100 for Nafion117), 1.008 is the formula weight of the proton in grams per mole, FW_{Ion} is the formula weight of the cation used, and SF is a scaling factor which accounts for any added electrode mass. For an unplated membrane, $SF = 1$; for the plated

IPMCs described above, the scaling factor is the weight fraction of Nafion within the sample (SF = 0.58 to 0.61).

The ion capacity of prepared samples can be determined from the weight difference of dry IPMCs containing different metal ions or by measuring the pH change of a salt solution after immersion of an H^+-form IPMC sample. A summary of ion capacity and hydration of Nafion versus IPMC samples is presented in Table 1 for an IPMC provided by the University of New Mexico's, Artificial Muscle Research Institute [Rashid and Shahinpoor, 1999]. Samples in the H^+-form contain considerably more water than the values given in Table 1, since a fully dried state cannot be easily attained [Gierke et al., 1981]. The data in Table 1 should be viewed as illustrative rather than definitive. Indeed, specific (e.g., per liter dry) ion content should be independent of the (monovalent, Table 1) cation form. Hence, the variation in the values of n_{ion} in Table 1, for example, is mainly due to experimental error as well as to possible mass changes during cation exchange.

6.4.3 Solvent Content and Swelling

The uptake of solvent from a dried IPMC sample is dependent on the method of solvation and the cation activity. The weight difference between dry and solvated samples indicates the mass of solvent taken up by each ion form. The ion exchange process is selective [Miyoshi et al., 1990; Iyer et al., 1992] and correlates with the extent of solvation.

Table 1: Illustrative results: ion exchange capacity of IPMC vs. Nafion117.

	Membrane	H^+	Rb^+	Cs^+	Tl^+	TMA^+	TBA^+
Eq. Wt. (W_e) *g* dry IPMC/mole ion	Nafion 117	1100	1184	1232	1303	1173	1341
	Metal	1929	2013	2061	2132	2002	2170
Hydration Volume Change (%)	Nafion 117	57%	29%	25%	31%	35%	28%
	Metal	53%	27%	24%	31%	33%	38%
One liter dry material hydrated to N-form has:							
n_{H2O} (moles)	Nafion 117	31.7	16.1	13.9	17.2	19.4	15.6
	IPMC	29.4	15.0	13.3	17.2	18.3	21.1
n_{ion} (moles)	Nafion 117	1.74	1.78	1.78	1.81	1.59	1.38
	IPMC	1.50	1.59	1.47	1.41	1.37	1.32
x_{H2O} (10^{-1})	Nafion 117	9.01	8.19	7.96	8.26	8.60	8.50
	IPMC	9.07	8.25	8.19	8.60	8.70	8.89
x_{M+} (10^{-2})	Nafion 117	4.95	9.05	10.2	8.70	7.01	7.52
	IPMC	4.63	8.74	9.04	7.02	6.49	5.57

Gebel and Pineri have also investigated the hydrative swelling of Nafion117 membranes [Gebel et al., 1993]. As well, Nafion hydration has been measured by quartz crystal gravimetric analysis [Shi and Anson, 1996] and infrared spectroscopy [Blanchard and Nuzzo, 2000; Ludvigsson et al., 2000]. We propose that the balance of osmotic pressures, electrostatic forces, and elastically induced interfacial stresses within the membrane determines the extent of solvation expansion. The elastic resistance (stiffness) of the backbone polymer is, in turn, dependent on the nature of the neutralizing cation. Dimensional measurements of IPMC samples indicate that solvent-induced swelling strains are smaller than in bare (nonplated) ionomer samples. Presumably, the stiffness of metal-coated layers restricts the expansion of IPMC samples and results in a smaller observed solvation.

It should be noted that hydration studies of Nafion-type polymers usually refer to three common states: the normal (N) form, in which dried samples have been hydrated at 25°C, the prepared (P) form, in which nondried hydrated H^+ samples have been ion exchanged at 25°C, or the expanded (E) form, in which dry ion-exchanged samples are hydrated at 100°C [Yeager et al., 1982]. Samples prepared in the expanded form can retain their swollen characteristics for long periods, often more than several weeks (Jeff McGee, personal communication; and McGee, 2002). Presumably, the hydration state of IPMC samples is affected by the hydration of H^+ samples near their glass transition temperature (104°C). This treatment should provide for the optimized water-swollen state for the H^+ form of the IPMC. The polymeric structure may thus become biased toward the ideal H^+ swollen state; subsequent ion exchanged states are then subject to the constraints imposed by this prepared state.

6.4.4 Ion Migration Rates

Xue et al. [1991] have shown that the diffusion of alkali metal ions through Nafion membranes varies with the ion used. At high concentration, it has been shown that the rate of diffusion is in the order $Li^+ < Cs^+ < Rb^+ < Na^+ < K^+$. Under applied voltages, cations within the membrane migrate toward the cathode. Ion motion occurs in tandem with water migration, either through primary solvation-shell migration of water or other solvent molecules, or through secondary electro-osmotic migration of water. These processes are determined by several factors, including the diffusion of water [Zelsmann et al., 1990] and migration of metal ions (e.g., sodium, cesium, and zinc) through Nafion membranes [Sodaye et al., 1996; Rollet et al., 2000].

6.4.5 Metal Content and Distribution

The distribution and morphology of deposited metal at the surface of IPMC materials has a significant effect on their actuation behavior. Many studies of metal deposition in IPMCs, including TEM analysis [Millet et al., 1989], x-ray microprobe analysis [Millet et al., 1992], and analysis of the surface area of

implanted electrodes have been performed [Chen and Chou, 1993]. Performance of IPMCs as actuators correlates with their surface morphology, with the best electrodes for IPMC actuators being those that exhibit the largest available surface area and greatest surface conductivity. Large surface areas can be attributed to the development of a highly dispersed particle distribution or the small size of individual metal particles (Fig. 4) or fine dendritic structure, as seen in Fig. 5, for gold plated Flemion. An indication of an electrode's surface area can be determined through measurement of an IPMC's behavior as a parallel plate capacitor. Moreover, surface conductivity can be measured directly (Nemat-Nasser and Wu, 2003a].

6.4.6 Modeling of Cluster Size

Hsu and Gierke [1982] proposed a model for ionic clustering in Nafion that describes the experimental data well. This model is based on elastic interaction between the fluorocarbon matrix and the ionic cluster. It ignores the electrostatic dipole interaction that is believed to be the driving force for the clustering [Eisenberg, 1970]. The electrostatic dipole interaction results in an increase in the stretching of the polymer chains, and thus an increase in the elastic energy of the matrix [Forsman, 1982]. Using a computer simulation, Datye et al. [1984] have shown that the electrostatic and elastic forces acting on the pendant ionic groups and their neutralizing counter-ions produce a dipole layer at the surface of an ionic cluster. Monte Carlo simulation [Datye and Taylor, 1985] has further revealed that the electrostatic energy of an ionic cluster in an ionomer is not very sensitive to the variation of the cluster shape. More recently, Li and Nemat-Nasser [2000] have sought to determine the cluster size and shape from free-energy minimization, taking into account the electrostatic dipole interaction energy, the elastic energy of the polymer chain reorganization during clustering, the cluster surface energy, and the electro-elastic interaction energy of the ionic clusters and the fluorocarbon polymer matrix. They also have examined the effect of the cluster morphology on the macroscopic electro-elastic and transport properties of the hydrated Nafion, using a micromechanical multi-inclusion model proposed by Nemat-Nasser and Hori [1993, 1999]. In what follows, the main results of this investigation that correspond to the average cluster size are summarized.

Consider a cluster of fixed radius containing a fixed number of dipoles. These dipoles are arranged on the cluster surface so as to minimize the free energy of the cluster. In such a situation, the spacing of the dipole pairs will be proportional to the cluster radius, while the corresponding orientation will be independent of the cluster radius. Thus the electrostatic energy of a cluster with N dipoles may be expressed as

$$U_{ele} = -g\frac{N^2}{4\pi\kappa_e}\frac{m^2}{r_c^3} = -\frac{N^2}{4\pi\kappa_e}\frac{m^{*2}}{r_c^3}, \tag{1}$$

where g is a geometric factor, depending only on the detailed arrangement of the dipoles on the cluster surface, r_c is the radius of the cluster, $m^* = \sqrt{g}m$ is the effective dipole moment, and κ_e is the effective electric permittivity of the water-swollen Nafion.

Datye et al. [1984] use a simple model of rubber elasticity to obtain the per-cluster elastic energy associated with clustering. The result can be expressed as

$$U_{ela} = \frac{3NkT}{< h^2 >}\left(\sqrt[3]{\frac{N\,EW}{\rho^* N_A}} - r_c \right)^2, \tag{2}$$

where k is Boltzmann's constant, T is the absolute temperature, $<h^2>$ is the mean square end-to-end chain length, EW is the equivalent-weight of Nafion (i.e., the weight in grams of dry polymer per mole of ion exchange sites), ρ^* is the effective density of the water-swollen Nafion membrane, and N_A is Avogadro's constant. In deriving Eq. (2) it is assumed that half of the pendant side-chain ions terminate on the same cluster while the remaining chains terminate on a nearest-neighbor cluster.

Finally, the surface energy of the cluster is expressed as

$$U_{sur} = 4\pi r_c^2 \gamma, \tag{3}$$

where γ is the surface energy density. Since the surface energy is composed of the hydrophilic energy between the water and the ion pairs, and the hydrophobic energy between the water and the fluorocarbon matrix, a small decrease in the surface energy density γ with an increase in the volume fraction of water is expected.

The number of clusters, n, per unit volume is given by

$$n = \frac{3(c_w + c_i)}{4\pi r_c^3}, \tag{4}$$

where $c_w = w/(1 + w)$ and $c_i = w'/(1 + w')$ are the volume fractions of the water and the ion exchange sites in the membrane, respectively; w denotes the water volume per unit dry polymer, and $w' = N_A V_i /(EW/\rho_d)$, with V_i being the volume of a single ion exchange site. Now, the total energy per unit volume can be calculated from the sum of the electrostatic dipole interaction energy, the elastic energy of the polymer chain reorganization, and the cluster surface energy. Minimizing this expression with respect to the cluster radius, Li and Nemat-Nasser [2000] obtained the following result for the cluster radius:

$$r_c^3 = \frac{(w+w')}{\rho_d}\left(1-\sqrt[3]{\frac{4\pi\rho_d}{3\rho^*(w+w')}}\right)^{-2}, \quad (5)$$

where $\rho^* = (\rho_d + w\rho_w)/(1 + w)$ is the effective density. Assuming $<h^2> = \beta\ EW$ [Forsman, 1986], Eq. (5) suggests that a plot of r_c^3 versus

$$\Phi = \frac{EW^2(w+w')}{\rho_d}\left(1-\sqrt[3]{\frac{4\pi\rho_d}{3\rho^*(w+w')}}\right)^{-2}$$

should be a straight line crossing the origin for all membranes of different equivalent weights, different cations, or water intake, with the slope given by $\gamma\beta/2N_AkT$. A typical value for Φ/EW^2 is 0.19 for w = 0.443. Using data from Gierke et al. [1981], Li and Nemat-Nasser show that a linear relation generally holds. Table 2 provides sample results reported by Gierke et al. [1981]. For more information and for the calculation of the cluster shape, see Li and Nemat-Nasser [2000].

Table 2: Cluster size of 1200 equivalent weight Nafion with different cations [Gierke et al., 1981].

Cation	H	Li	Na	K	Rb	Cs
Dry density (g/cm^3)	2.075	2.078	2.113	2.141	2.221	2.304
Volume gain (%)	69.7	61.7	44.3	18.7	17.9	13.6
Cluster diameter (nm)	4.74	4.49	4.21	3.45	3.56	3.5

6.4.7 Stiffness

Nafion polymers are viscoelastic, exhibiting first-order tensile moduli from 50–1500 MPa and greater. The large variance in stiffness is primarily due to the presence or absence of solvent, but the nature of the countercation present is a significant stiffness factor, especially for dry samples. The variation in stiffness is attributed to the action of ions within the membrane increasing stiffness by acting as cross-linking agents [Eisenberg et al., 1996]. Ionomeric polymers containing polyvalent cations may act as noncovalent cross-linking agents, binding multiple anionic side-chains by ligand coordination. Similarly, monovalent cations such as alkali metals or tetraalkylammonium salts may serve to cross-link ionomers via dipolar interactions between individual salt pairs.

The stiffness of dry IPMC samples correlates with the radius of the alkali metal countercation (Li^+, Na^+, K^+, Rb^+, Cs^+, and Tl^+). Smaller cations may more

closely approach the sulfonate anion, yielding a smaller ion pair dipole [Gejji et al., 1997]. Larger dipoles in interaction will require a greater energy for reorganization. This can result in a larger observed stiffness of the material.

The Young's moduli of IPMC materials for a variety of cations have been determined. These values were compared to the same-cation unplated ionomer samples. Measurements were obtained using a mini-load frame developed in the author's lab by Jon Isaacs (Fig. 7). Some typical results of these experiments are summarized in Table 3. In these tests, the same sample is sequentially neutralized by the indicated countercations, and tested. Therefore, the differences in the measured stiffness are due to the effect of the cations. Similar measurements are performed on several other IPMCs that have been produced by Shahinpoor and coworkers using new processing techniques, as well as on Flemion and Flemion-based IPMCs that were provided by Dr. Kenji Asaka. Additional results are given later on in this section; see also Nemat-Nasser [2002], Nemat-Nasser and Wu [2003a,b], Nemat-Nasser and Zamani [2003].

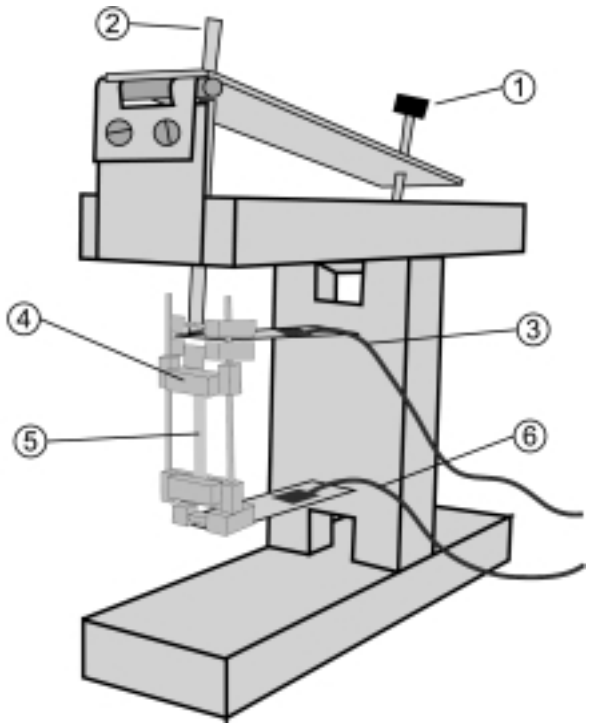

Figure 7: Diagram of mini-load frame. (1) Force adjuster, motorized; (2) force arm; (3) displacement gauge; (4) sample clamps; (5) IPMC sample; (6) load-displacement gauge.

Table 3: Stiffness of bare Nafion and IPMC samples in dry and hydrated form for indicated cations.

	Nafion 117		IPMC	
Ion	wet	dry	wet	dry
H			140	340
Li	70	300	90	650
Na	80	500	90	
K	120	1010	170	–
Rb	–	850		–
Cs	210	1200	190	1270
Tl		750	190	1300
TMA	110	760	140	830
TBA	–	–	130	1400

The measured axial stiffness of Nafion and IPMC samples in dry and solvated states allows estimation of the corresponding bending stiffness. An expression for the extensional stiffness of the IPMC in terms of the Young's moduli of bare ionomer and the surrounding thin surface electrodes is presented. The result is used to estimate the bending stiffness of the IPMC. Since the extensional stiffness is also directly measured, the model estimate of the extensional stiffness of the IPMC provides an assessment of the effective stiffness of the plating region. The thin metal electrodes contain numerous microcracks, and a diffuse metal particle distribution or a fine dendritic metal structure provides for an electrode with large surface area, as shown in Figs. 4 and 5. Hence, only an effective extensional modulus can be assigned to these regions within the IPMC. By direct measurement of the extensional stiffness of the bare membrane and the IPMC, the effective stiffness may be calculated and used as a measure of the effectiveness of the plating procedure.

In a recent work, Nemat-Nasser [2002] provides a micromechanical model to estimate the extensional stiffness of both the membrane and the corresponding IPMC as functions of the solvation level for each neutralizing countercation. The model is based on the observation that a dry sample of a bare polymer or an IPMC immersed in a solvent absorbs the solvent until the resulting pressure within its clusters is balanced by the elastic stresses that are consequently developed within its backbone polymer membrane. From this observation then the stiffness of the membrane is calculated as a function of the solvent uptake for various cations. In this calculation, first the balance of the cluster pressure and the elastic stresses for the bare polymer (no metal plating) is considered, and then the results are used to calculate the stiffness of the corresponding IPMC by

including the effect of the added metal electrodes. The procedure also provides a way of estimating many of the microstructural parameters that are needed for the modeling of the actuation of the IPMCs. Since, for both the Nafion- and Flemion-based IPMCs, the overall stiffness of both bare membrane and the corresponding IPMCs has been measured directly as a function of the hydration (or solvation by other solvents), the basic assumptions and the results can be subjected to experimental verification [Nemat-Nasser, 2002; Nemat-Nasser and Wu 2003a; Nemat-Nasser and Zamani, 2003].

6.4.7.1 Extensional Stiffness of Bare Polymer

The stresses within the bare polymer may be estimated by modeling the polymer matrix as an incompressible elastic material [Treolar, 1958; Atkin and Fox, 1980]. It will prove adequate to consider a neo-Hookean model for the matrix material, where the principal stresses σ_I are related to the principal stretches λ_I by

$$\sigma_I = -p_0 + K\lambda_I^2; \tag{6}$$

here, $p_0(w)$ is an undetermined parameter (pressure) to be calculated from the boundary data; in spherical coordinates, $I = r, \theta, \varphi,$ for the radial and the two hoop components; and $K = K(w)$ is an *effective stiffness*, which depends on the cation type and its concentration, and on the solvent uptake, *w*.

The aim is to calculate K and p_0 as functions of *w* for various ion-form membranes. For this, examine the deformation of a unit cell of the solvated polyelectrolyte by considering a spherical cavity of initial (dry state) radius a_0 (representing a cluster), embedded at the center of a spherical matrix of initial radius R_0, and placed in a *homogenized solvated membrane*, referred to as the *matrix*. Assume that the stiffness of both the spherical shell and the homogenized matrix is the same as that of the (yet unknown) overall effective stiffness of the solvated membrane. For an isotropic expansion of a typical cluster, the two hoop stretches are equal, $\lambda_\varphi = \lambda_\theta$, and incompressibility yields $\lambda_r \lambda_\theta^2 = 1$, leading to

$$\sigma_r(r_0) = -p_0 + K\lambda_\theta^{-4}(r_0), \quad \sigma_\theta(r_0) = -p_0 + K\lambda_\theta^2(r_0), \tag{7}$$

where r_0 measures the initial radial distance from the center of the cluster. The basic observation is that the *effective elastic resistance* of the (homogenized solvated) membrane balances the cluster's pressure, p_c, which is produced by the combined osmotic and electrostatic forces within the cluster.

Upon solvation from an initial state with w_0 solvent uptake, material points initially at r_0 move to *r*,

$$r^3 = r_0^3 + a_0^3(w/w_0 - 1), \quad n_0 = (a_0/R_0)^3, \quad w_0 = n_0/(1-n_0), \tag{8}$$

where n_0 is the initial porosity (volume of saturated or dry void divided by total volume). The radial and hoop stresses at an initial distance of r_0 from the cluster center then become

$$\begin{aligned} \sigma_r(r_0) &= -p_0 + K[(r_0/a_0)^{-3}(w/w_0 - 1) + 1]^{-4/3}, \\ \sigma_\theta(r_0) &= -p_0 + K[(r_0/a_0)^{-3}(w/w_0 - 1) + 1]^{2/3}. \end{aligned} \tag{9}$$

The radial stress, σ_r, must equal the pressure, p_c, in the cluster, at $r_0 = a_0$, i.e., $\sigma_r(a_0) = -p_c$. In addition, the volume average of the stress tensor, taken over the entire membrane, must vanish in the absence of any externally applied loads, i.e.,

$$\frac{1}{V_{dry}} \int_{V_{dry}} \frac{1}{3}(\sigma_r + 2\sigma_\theta)\, dV_{dry} - w p_c = 0. \tag{10}$$

This is a *consistency condition* that to a degree accounts for the interaction among clusters. These conditions are sufficient to yield the undetermined pressure p_0, and the stiffness, *K*, in terms of *w* and w_0, for each ion-form bare membrane.

To estimate the cluster pressure, p_c, note that in the absence of an applied electric field, this pressure consists of an osmotic part, $\Pi(M^+)$, and an electrostatic (dipole-dipole interaction) part, p_{DD}, i.e., $p_c = \Pi(M^+) + p_{DD}$, where M^+ stands for the considered cation. Detailed calculations are given by Nemat-Nasser [2002]. The final expression is

$$p_c = \frac{2\rho_B RT\phi}{EW_{Ion} w} + \frac{1}{3\kappa_e}\left(\frac{\rho_B F}{EW_{Ion}}\right)^2 \frac{\pm\alpha^2}{w^2}, \tag{11}$$

where *F* is Faraday's constant (96,487 C/mol), ρ_B is the dry density of the bare membrane, *R* = 8.31 J/mol/K is the gas constant, *T* (= 300 K) is the test temperature, EW_{Ion} is the equivalent weight of bare membrane, $\kappa_e = \kappa_e(w)$ is the effective electric permittivity in the cluster, $\alpha = \alpha(w)$ is an effective dipole length, and ϕ is the osmotic coefficient. From $\sigma_r(a_0) = -p_c$ [Eqs. (10), and (11)], it follows that

$$K(w)=p_c\frac{(1+w)}{w_0 I_n-\left(\frac{w_0}{w}\right)^{4/3}},\quad I_n=\frac{1+2An_0}{n_0(1+An_0)^{1/3}}-\frac{1+2A}{(1+A)^{1/3}}$$

$$p_0(w)=K\left(\frac{w}{w_0}\right)^{-4/3}+p_c,\quad A=\frac{w}{w_0}-1. \tag{12}$$

It turns out that the electrostatic forces are a dominating element in this calculation, with the dielectric properties of the solvent playing an important role. Consider for illustration, water as the solvent. As part of the hydration shell of an ion, water has a dielectric constant of 6, whereas as free molecules, its room-temperature dielectric constant is about 78. The number of mole water per mole ion within a cluster is

$$m_w=\frac{EW_{\text{Ion}}w}{36\rho_B}. \tag{13}$$

Hence, when the water uptake is less than *CN* moles per mole of ion within a cluster, set $\kappa_e=6\kappa_0$, where $\kappa_0=8.85\times10^{-12}$ F/m is the electric permittivity of the free space and *CN* is the coordination number (number of water molecules per ion in bulk). On the other hand, when more water is available in a cluster, i.e., when $m_w > CN$, calculate κ_e as follows:

$$\kappa_e=\frac{7+6f}{7-6f}6\kappa_0,\quad f=\frac{m_w-CN}{m_w}, \tag{14}$$

where $(14)_1$ is obtained as a special case of Eq. (60) which is discussed in Sec. 6.5.7.9. As a first-order approximation, assume α^2 in Eq. (11) is linear in *w* for $m_w \le CN$,

$$\pm\alpha^2=a_1w+a_2, \tag{15}$$

and estimate a_1 and a_2 from the experimental data. For $m_w > CN$, assume that the distance between the two charges forming a pseudo-dipole is controlled by the effective electric permittivity of their environment (i.e., water molecules), and set (measured in meters)

$$\alpha=10^{-10}\frac{7+6f}{7-6f}(a_1w+a_2)^{1/2}, \tag{16}$$

which is obtained from Eq. $(15)_1$ by setting $\kappa_e = 10^{-10}(a_1 w + a_2)^{1/2}$.

Figure 8 shows the experimentally measured Young modulus of the bare Nafion-117 and the corresponding IPMC, in Cs^+-form. The Young's modulus Y_B of the hydrated strip of bare polymer relates to the stiffness K, by $Y_B = 3K$, based on incompressibility. The lower solid curve (bare Nafion) is obtained from Eq. (13), using the following parameters: FW_{Cs+} = 132.91 g/mol, ρ_B = 2.16 g/cm^3 (measured dry density), n_0 = 0.01, and ϕ = 1. The values of a_1 and a_2 in Eq. (A9) are obtained as 1.6383 × 10^{-20} and -0.0807 × 10^{-20} (in m^2), respectively, by setting Y_B = 1130 MPa for w = 0.02 and Y_B = 158 MPa for w = 0.42. Figure 9 shows the experimentally measured Young's modulus of the bare Flemion-1.44 and the corresponding IPMC in Cs^+-form. The model results (lower solid curve), are obtained based on: EW_{H+} = 694.4 g/mol, ρ_B = 2.19 g/cm^3, and a_1 = 0.8157 × 10^{-20} and a_2 = –0.0606 × 10^{-20}, obtained by setting Y_B = 1006 MPa for w = 0.036 and Y_B = 147 MPa for w = 0.54.

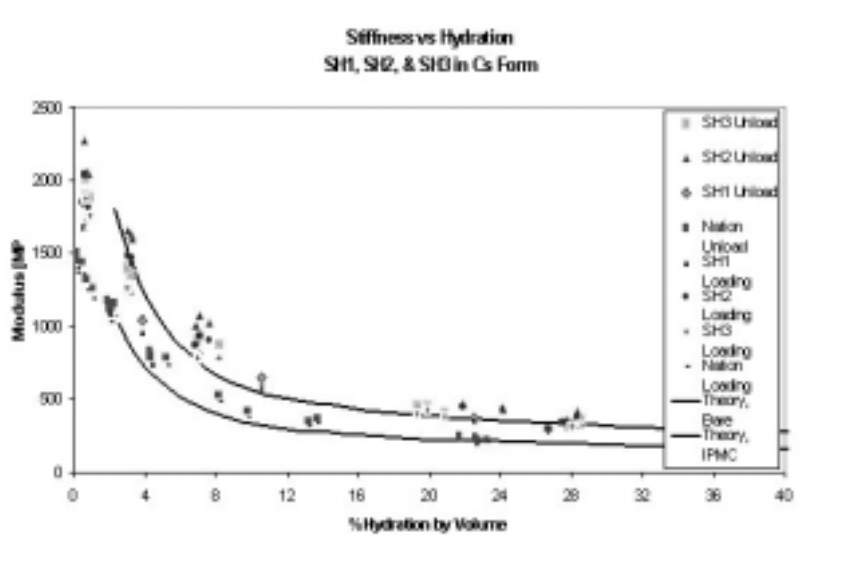

Figure 8: Stiffness versus hydration of Nafion ionomer (lower data points and the solid curve) and IPMCs (upper data points and the solid curve) in Cs+-form.

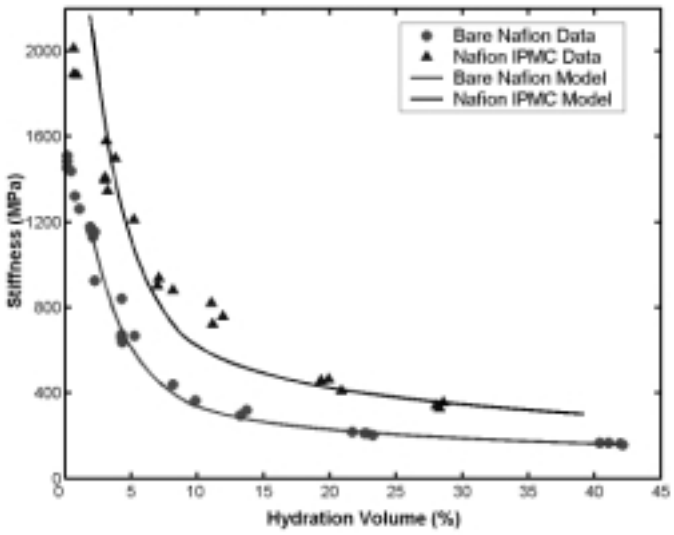

Figure 9: Stiffness versus hydration of Flemion ionomer (lower data points and the solid curve) and IPMCs (upper data points and the solid curve) in Cs+-form.

6.4.7.2 Extensional Stiffness of IPMC

To include the effect of metal plating, assume a uniaxial stress state and by volume averaging obtain

$$\bar{\varepsilon}_{IPMC} = f_{MH}\bar{\varepsilon}_M + (1 - f_{MH})\bar{\varepsilon}_B,$$
$$\bar{\sigma}_{IPMC} = f_{MH}\bar{\sigma}_M + (1 - f_{MH})\bar{\sigma}_B, \quad f_{MH} = \frac{f_M}{1+w}, \tag{17}$$

where the barred quantities are the average uniaxial values of the strain and stress in the IPMC, metal, and bare polymer, respectively, and f_M is the volume fraction of the metal plating in a dry sample, given by

$$f_M = \frac{(1-SF)\rho_B}{(1-SF)\rho_B + SF\rho_M}, \tag{18}$$

where ρ_M is the mass density of the metal plating and *SF* is the scaling factor, representing the weight fraction of dry polymer in the IPMC. The average stress in the bare polymer and in the metal are assumed to relate to the overall average stress of the IPMC, by

$$\bar{\sigma}_B = A_B \bar{\sigma}_{IPMC}\,,\ \bar{\sigma}_M = A_M \bar{\sigma}_{IPMC}\,, \tag{19}$$

where A_B and A_M are the concentration factors. Setting $\bar{\sigma}_B = Y_B \bar{\varepsilon}_B$, $\bar{\sigma}_M = Y_M \bar{\varepsilon}_M$, and $\bar{\sigma}_{IPMC} = Y_{IPMC} \bar{\varepsilon}_{IPMC}$, obtain

$$\bar{Y}_{IPMC} = \frac{Y_M Y_B}{BA_B Y_M + (1 - BA_B) Y_B}\,,$$
$$B = \frac{(1+\bar{w})(1-f_M)}{1+\bar{w}(1-f_M)},\ w = \bar{w}(1-f_M)\,. \tag{20}$$

Here, Y_B is evaluated at solvation of $\bar{w}$ when the solvation of the IPMC is *w*. The latter is measured directly at various hydration levels.

The result for the Nafion-based IPMC is shown in Fig. 8 (the upper solid curve), using a scale factor of 0.6, and ρ_M = 20 g/cm^3 for the combined overall density of gold and platinum, with Y_M = 75 GPa (the results are insensitive to this quantity) and A_B = 0.55. For the Flemion-based IPMC, the same procedure is used with *SF* = 0.54, ρ_M = 19.3 g/cm^3 (for gold), Y_M = 75 GPa, and A_B = 0.5, leading to the results given in Fig. 9 by the upper solid curve.

6.4.7.3 Bending Stiffness of IPMC

For a given (antisymmetric) axial stress distribution, $\sigma(x)$, over a cross section of an IPMC strip, the bending moment *M*, acting at that cross section is given by (see Fig. 10)

$$M = \int_{-H}^{H} \sigma(x) x dx = 2\int_{0}^{H} Y(x)\varepsilon(x) x dx. \tag{21}$$

Since IPMCs are very thin, the Euler beam theory applies. The strain $\varepsilon(x)$ is linear over the cross section of the strip,

$$\varepsilon(x) = \varepsilon_{\max} \frac{x}{H}, \tag{22}$$

and hence Eq. (21) becomes

$$M = \frac{2\varepsilon_{\max}}{H}\int_{0}^{H} Y(x)\, x^2 dx = \frac{2}{3}\varepsilon_{\max} H^2 (3\bar{Y}_{IPMC} - 2Y_B) + O(t/H)^2\ , \tag{23}$$

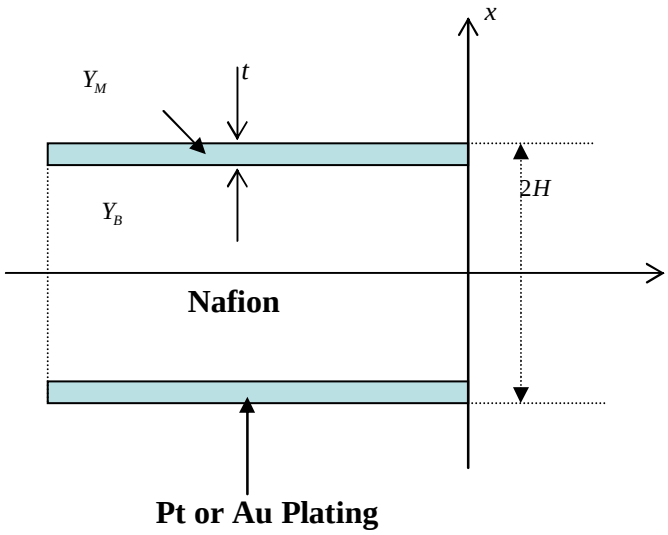

Figure 10: Edge-on diagram of IPMC used in modeling force output.

where $O(t/H)^2$ indicates (negligible) terms of the second order and higher in the small parameter t/H.

If we define the effective bending stiffness $\overline{Y}$ as the stiffness of a uniform strip having the same geometry, to the first order in (t/H) the effective Young's modulus corresponding to bending is given by $\overline{Y} \equiv 3\overline{Y}_{IPMC} - 2Y_B$.

6.4.8 Internal Force in IPMCs

The bending moment M can be used as a measure of the internal forces that produce a corresponding displacement. The displacement of a cantilever strip subjected to an electric potential can be measured directly. From this, ε_{max} and the corresponding bending moment along the length of the strip can be calculated.

Let the radius of curvature at a typical point along the strip be denoted by R_0 before the application of a voltage, and by R afterwards (see Fig. 11). For an element of the strip initially subtended by angle $d\theta_0$, which upon pure bending changes to $d\theta$, the maximum strain at the top (tension, +) and at the bottom (compression, –) are equal to

$$\varepsilon_{max} = \frac{R \pm H}{R_0 \pm H}\frac{d\theta}{d\theta_0} - 1 = \pm H\left(\frac{1}{R} - \frac{1}{R_0}\right) + O\left(\frac{H}{R}\right)^2, \qquad (24)$$

where the plus sign corresponds to the upper, and the minus sign to the lower edge of the cross section.

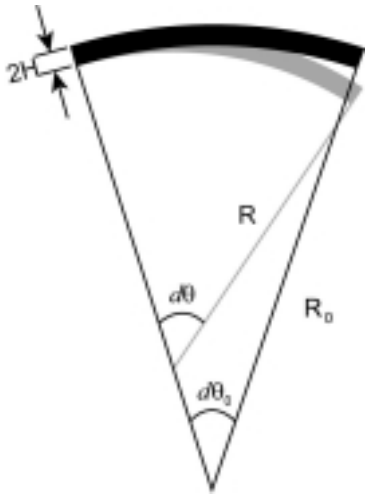

Figure 11: Pure bending of an element of an IPMC strip corresponds to a change in the local radius of curvature.

For small deflection of the strip, observed when the applied voltage is below that required for water electrolysis, we may use the following approximation:

$$\frac{1}{R} \approx \frac{d^2u}{dz^2}, \quad \frac{1}{R_0} \approx \frac{d^2u_0}{dz^2}, \tag{25}$$

where u and u_0 are the deformed and initial deflections of the strip, respectively. From Eqs. (24) and (25) it follows that, for a cantilevered strip,

$$\varepsilon_{max} = \pm \frac{2H}{z^2}(u - u_0), \tag{26}$$

where z measures length along the strip from its fixed end.

Assume that the internal forces generated in the strip are represented by equivalent forces that are concentrated at a distance $H - t$ from the centerline of the strip, as shown in Fig. 7. We may then represent these forces by

$$\begin{aligned} F &= \frac{M}{2(H-t)} = \frac{M}{2H}\left(1 + \frac{t}{H}\right) + O\left(\frac{t}{H}\right)^2 \\ &= \frac{1}{3}\varepsilon_{max} H\left(1 + \frac{t}{H}\right)(3\bar{Y} - 2Y_B) + O\left(\frac{t}{H}\right)^2, \end{aligned} \tag{27}$$

where ε_{max} is given by Eq. (26), and F is the resultant internal force producing the bending moment M necessary to induce the displacement $u - u_0$.

As has been pointed out before, the stiffness of the IPMC strip depends on the nature of the countercation and the level of solvation. Considerably greater internal forces are required for Cs^+-form IPMCs to yield the same induced displacement $u - u_0$, as compared with Li^+ or Na^+.

Other methods have been used to estimate the force output. These methods usually involve the measurement of total tip deflection and determination of the required restoring force. This method has been used by Asaka and Oguro [2000], Bar-Cohen et al. [1999b], McGee [2002], Mojarrad and Shahinpoor [1996, 1997], and Shahinpoor [1999]. These materials can be actuated at tens of Hz, depending on the sample geometry and boundary conditions. This limiting bandwidth factor will determine the ultimate power that can be generated by IPMC materials [Shahinpoor et al., 1997].

6.5 Actuation Mechanism

Several models for the mechanism of IPMC actuation have been presented. De Gennes et al. [2000] have suggested a model that incorporates water pressure gradients and the overall electric field as thermodynamic forces that induce ion/water fluxes as primary mechanisms for actuation. Shahinpoor et al. offer an electromechanical model for IPMC motion [Shahinpoor, 1995; Shahinpoor and Thompson, 1995; Shahinpoor, 1999], and Asaka and Oguro [2000] have proffered a model by which water flow, induced by pressure gradients and electro-osmotic flow, may generate swelling stresses to drive actuation. Nemat-Nasser and Li [2000] presented a model that includes ion and water transport, electric field, and elastic deformation, emphasizing that ion transport may dominate the initial fast motion of IPMC materials. More recently, Nemat-Nasser [2002] has examined in some detail hydraulic, osmotic, electrostatic, and elastic forces that may affect actuation of fully hydrated Nafion-based IPMCs in various cation-forms, concluding that the electrostatic and osmotic forces within the clusters and the elastic resisting force of the backbone ionomer basically control the actuation, with water flowing into or out of the clusters as a response to these forces. Direct measurement of cation charge accumulation in the cathode region of an IPMC strip has decidedly shown that this continued charge accumulation is accompanied by cathode contraction which produces bending towards the cathode [Nemat-Nasser and Wu, 2003a]. This is illustrated in Fig. 12, from Nemat-Nasser and Wu [2003a]. As is seen, back relaxation occurs soon after actuation has begun while cations are migrating into the cathode side, presumably carrying with them their hydration water molecules.

In this section, we present a detailed description of the phenomenon of actuation under a 1 to 3V applied dc signal. Following this, we present a summary of the requisite points of the Nemat-Nasser and Li [2000] and Nemat-Nasser [2002] model for IPMC sensing and actuation, including comments as

appropriate regarding the relationship of this model to other proposed models. We discuss both the initial fast motion as well as the subsequent relaxation aspects of the actuation of Nafion-based IPMCs. First, we provide an outline of the primary physical components of the model. Then, we present specific details supporting the model as have been worked out to date, including new observations and results. Numerical results and comparison with experimental data are reported elsewhere [Nemat-Nasser, 2002].

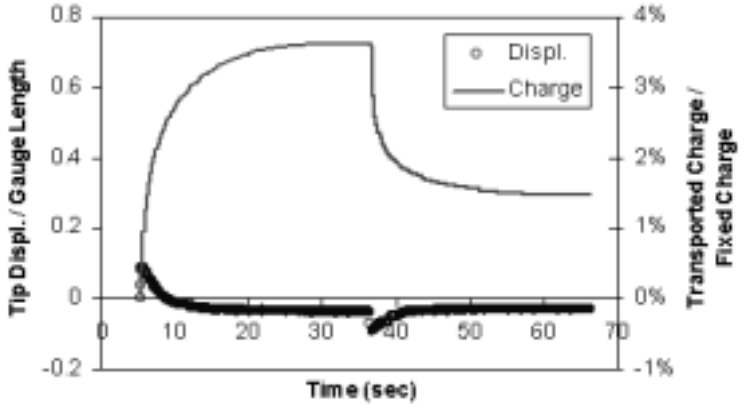

Figure 12: Tip displacement and accumulated charge versus time for a Nafion-based IPMC in Na^+-form, with 1.5V DC applied and then shorted.

6.5.1 Model Summary

Consider a model of an IPMC, where the hydrophobic backbone fluorocarbon polymer is separated from the hydrophilic clusters, as schematically represented in Fig. 13. The anions within the clusters are attached to the fluorocarbon matrix, while under suitable conditions the associated unbound cations may move within the water that permeates the interconnected clusters. Under an electric field, cations redistribute and migrate toward the cathode. This redistribution produces several significant changes in the local properties of the composite, specific to the anode and cathode. These changes form the basis for our model of IPMC actuation, and are suitable for explaining the observed actuation and subsequent relaxation of IPMC materials. Our research is aimed at quantifying each effect and determining which are best suited to improving the actuating properties of IPMCs.

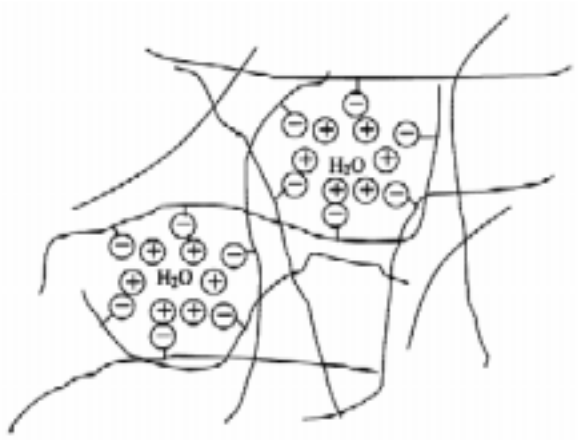

Figure 13: Schematic depiction of polymer domains within IPMC materials.

At the *anode*, the application of the electric field results in depletion of cations from their clusters. We refer to this thin layer as the *anode boundary layer*. The reduction in cation concentration may produce any of the following effects within the anode layer:

(1) A decrease in the effective stiffness of the polymer.
(2) A repulsive electrostatic force among the fixed anions within each cluster, which tends to increase the average cluster volume and also relax the prestretched polymer chains between adjacent clusters. This leads to an increase in the associated entropy and a decrease in the elastic energy of the polymer; polymer chains coil back to lower energy states.
(3) Reorientation of the remaining water in the clusters, which tends to increase the effective electric permittivity of the clusters and hence reduce the electrostatic repulsive forces among the fixed charges within each cluster.
(4) A decrease in the osmotic pressure inside the clusters, due to the reduced ion concentration.
(5) Removal or addition of water (solvent), in response to reduction or increase in the average volume of the clusters.

At the *cathode*, another boundary layer is formed in which local clusters contain an excess in the cation concentration. We refer to this thin layer as the *cathode boundary layer*. The excess cations may produce any of the following effects within the cathode boundary layer:

(1) An increase in the effective stiffness of the polymer.
(2) A change in the attractive electrostatic force within each cluster, which tends to hold the fixed anions more tightly within the cluster, decreasing the associated entropy and increasing the elastic energy of the polymer.

(3) A reduction in the effective electric permittivity of the clusters, which tends to increase the electrostatic forces between cations and the fixed anions within each cluster.
(4) An increase in the osmotic pressure within the clusters, due to the increased ion concentration.
(5) A reorganization of ions in cation-rich clusters, through interaction with fixed anions, depending on the nature of the cations (whether soft, as Tl^+, or hard, as H^+) and the anions (whether strongly acidic, as sulfonate, or weakly acidic, as carboxylate), leading to changes in the corresponding electrostatic interaction forces.
(6) Removal or addition of water (solvent), in response to reduction or increase in the average volume of the clusters.

As is shown in Sec. 6.4.7, the stiffness of the IPMC membrane is critically affected by the nature of the bound cations. Effects (1) and (2) pertain to this fact: the greater the interaction forces between the cations and the fixed anions within the clusters, the greater the resulting stiffness of both Nafion and IPMCs in both solvated and dry forms. Therefore, it is reasonable to expect that removal of all the cations from the clusters would lead to a decrease in the corresponding stiffness, and that their addition would tend to have a reverse effect. Furthermore, the anion-cation coupling within the clusters provides a pseudo cross-linking and a structured arrangement with concomitant increase in the internal energy and decrease in the entropy of the system. Effects (1) and (2) are therefore closely connected. In addition, reorganization of ions in cation-rich clusters, may occur depending on the nature of the cations (whether soft, as Tl^+, or hard, as H^+) and that of the fixed anions (whether strongly acidic, as sulfonate, or weakly acidic, as carboxylate), leading to changes in the corresponding electrostatic interaction forces. This reorganization appears to be at the heart of the mechanism responsible for the observed large and slow relaxation motion of the Nafion-based IPMCs that contain alkali-metal cations, as well as soft cations such as Tl^+; see Fig. 14.

Effect (3) stems from the fact that free water exhibits a dielectric constant of 78 at room temperature. Such a high dielectric constant reflects the ability of water, a polar molecule, to reorient to oppose applied electric fields. Waters of hydration, bound to ions in the solvent, are restricted by this association and exhibit a reduced effective dielectric constant, on the order of 6 at room temperature [Bockris and Reddy, 1998]. Similar comments apply to other polar solvents, such as ethylene glycol, glycerol, and various crown ethers [Nemat-Nasser and Zamani, 2003].

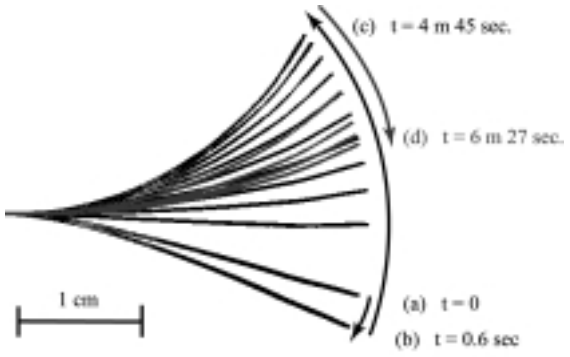

Figure 14: Representation of IPMC actuation. Sample is in the thallium (I) ion form, and a 1-V dc signal is suddenly applied and maintained during the first five minutes, after which the voltage is removed and the two electrodes are shorted. Initial fast bend toward the bottom (anode) occurs during the first 0.6 sec, followed by a long relaxation to upward (cathode) over 4.75 min. Upon shorting, the sample displays a fast bend in the same upward direction (not shown), followed by slow downward relaxation during the next 1.75 min.

Some of the primary solvation molecules may be carried away from or into the clusters by the cations, producing an osmotic imbalance and hence some solvent exchange with the surrounding bath. This principle is not without exception, as tetrabutylammonium cations carry no hydration waters, and H^+ migrates via the *Grotthuss mechanism*, an entirely different mechanism of ion migration that stems from the hydrogen-containing nature of water. This mechanism does not involve diffusion, but rather hopping of H^+ from one water molecule to another at the speed of about 100 μm per μs. In this event, H^+ does not transport any water with it, and the *transient* process is so fast that no significant diffusion can accompany it. (A steady-state proton transport through a membrane may involve some water transport, but not in the transient Grotthuss mechanism). In addition, the proton has a large number of tightly held (via electrostriction) hydration water molecules, about 10 H_2O per each H^+. As an H^+ leaves a cluster under the action of a suddenly applied electric field, its tightly held hydration water molecules are left behind, expanding up to possibly 10% in volume. Nevertheless, experiments show an initial fast response (albeit limited) for protonated Nafion-based IPMCs, similar to that for other metal cations (i.e., towards the anode), followed by a similar reverse slow relaxation. This suggests that effects (1) to (3) [rather than the often-assumed hydraulic water-pressure effect] are dominant in producing the initial fast response of the IPMC for certain cations, as well as its subsequent back relaxation. In general, all listed effects are coupled and occur in tandem.

Experimental observations suggest that the slow relaxation is dominated by effect (5) within the cathode boundary layer, where a redistribution of the excess cations occurs at a slower rate than the rate of cation supply. Recent experiments

by Nemat-Nasser and Wu have shown that with a suitably slow voltage buildup, the fast initial motion towards the anode of Nafion-based IPMCs can be precluded for cations that otherwise display substantial initial quick motion in that direction, e.g., sodium. The slow potential buildup allows for reconfiguration of the cations within the cathode clusters, as fewer cations move into these clusters, creating contractive forces that reduce the cluster size and actually expel solvent from these clusters. This process is accompanied by the solvent diffusion into the anode. Indeed, experiments using glycerol as the solvent show that, while the anode surface is drying during bending relaxation towards the cathode, droplets are appearing on the cathode surface.

The two boundary layers, together with their corresponding charged electrodes, form two *double layers*, one on the anode side and the other on the cathode side. These double layers provide *shielding* of the remaining part of the IPMC from the effects of the applied electric potential. This suggests that essentially all critical processes occur at the two boundary layers, especially the cathode boundary layer. Each boundary layer has its own distinct characteristics.

In passing, we mention that a fast motion in the same (cathode) direction follows the slow reverse motion of Nafion-based IPMCs, once the two electrodes are shorted. This fast motion is then followed by a slow relaxation in the opposite direction, i.e., towards the initial state of the sample. Here again, this fast motion towards the cathode is due to the rather quick redistribution of the cations, which may or may not (e.g., for H^+) involve water transport. The subsequent slow relaxation towards the anode is caused by the reconfiguration of the cations within the clusters, and the osmotic water transport due to stiffness and ion concentration changes.

6.5.2 Actuation Process

Asaka et al. [1995] describe the actuation of a Pt-IPMC sample in the sodium form. This sample "quickly bends to the anode side and bends back to the cathode side gradually." The initial deflection observed was sufficient to move the tip horizontally a distance approximately 7% of the overall length of the sample. This initial deflection is fast, achieving full displacement within 100 ms. We have made similar observations for several cations, including Tl^+, as shown in Fig. 14.

Substitution of alkali metal cations, as well as tetramethylammonium (TMA) and tetrabutylammonium (TBA) cations yields different deflection speeds and displacements for the same IPMC. The relaxation phenomenon varies widely by ion, with samples such as thallium displaying relaxation displacements greater than five times the initial actuating displacement (Fig. 14).

In the following section, we present the basic concepts and equations necessary for modeling the actuation phenomena observed in IPMCs, starting with an estimate of the internal forces induced by the hydration of a dry IPMC.

6.5.3 Osmosis-Induced Pretension

Consider a *dry* strip of IPMC neutralized by a given cation, M^+. When this strip is immersed in water, osmotic pressures develop in order to reduce the concentration of anions and cations within the clusters. This pressure induces hydration within the sample. As water diffuses into the clusters, the clusters dilate until the pressure induced by the elasticity of the surrounding hydrophobic matrix material balances the osmotic pressure that tends to add water to each cluster and further dilute the salt concentration within each cluster. The pressure in the clusters produces tension within the surrounding backbone polymer matrix. In the absence of external forces other than the surrounding water pressure, the *average* (equilibrium) hydrostatic tension in the fluorocarbon-backbone matrix material can be calculated, as follows, where, to be specific, Nafion-based IPMCs with water as solvent are considered.

Assuming a pure water bath, denote the chemical potential of the water external to the IPMC, by $\mu_w(p)$, where p is the water pressure used as the reference pressure. Let the volume fraction of the IPMC's hydration water at *equilibrium* be denoted by w and denote by $M_{SO_3^-}$ the concentration of sulfonate ions in mole per cubic meter of dry IPMC; here w is the (total) volume of the intake water per unit volume of the dry IPMC. The total ion concentration (measured per unit volume of water) is $n(\nu M_{SO_3^-}) = \nu M_{SO_3^-}/w$, where ν is the number of ions formed when one molecule of salt dissolves (ν = 2 for alkali sulfonates). Since the molar concentration of pure water is $10^6/18$ mol/m^3, the mole fraction of water in the clusters is given by

$$x(H_2O) = (10^6/18)/(10^6/18 + \nu M_{SO_3^-}/w). \tag{28}$$

The corresponding osmotic pressure in MPa, $\Pi(M^+)$, associated with the cation M^+ is now given by

$$\Pi(M^+) = -\frac{RT}{18} g \ln\left[x(H_2O)\right] = \frac{RT}{1000}\phi\nu\, m, \tag{29}$$

where ϕ is the osmotic coefficient of the metal sulfonate salt at the molality m in the cluster environment, (i.e., m is the ion concentration in mole per kilogram solvent); and g is the "rational" osmotic coefficient [Robinson and Stokes, 1965]. The rational osmotic coefficient, g, relates to ϕ approximately by $g = \phi(1 + 0.009\,\nu m)$. Except for the value of these coefficients, Eq. (29) for a given IPMC depends on the volume fraction of water, w, only. Metal salts of trifluoromethanesulfonic acid (CF_3SO_3H, triflate) can be used as model compounds for ionomer-bound sulfonic acid groups [Bonner, 1981]. Table 4 gives estimates of the osmotic pressure $\Pi(M^+)$ for several cations, assuming the

ideal situation where $\phi = 1$. As is seen, the smaller the volume fraction of water, the greater is the resulting osmotic pressure. However, since for $\phi = 1$, Eq. (29) becomes independent of the nature of the cations, it may be concluded that the substantial differences in the osmotic pressures reported in Table 4 are basically due to the (elastic) resistance provided by the fluorocarbon matrix material. This observation is in line with the differences in the measured stiffness of the composite reported in Table 3 for various cations. Similar differences are observed for plain Nafion. Hence, cations associated with smaller hydration volumes provide greater pseudo-cross-link forces that result in stiffer composites. It is, therefore, this stiffness that defines the level of hydration associated with each cation. The stiffer membrane would thus be under greater nominal tension when hydrated. The average and the nominal stresses carried by the backbone polymer are computed, as follows; see also Sec. 6.5.7.9.

The stress in the clusters is hydrostatic compression, given by $\boldsymbol{\sigma}_0 = -\Pi(M^+)\,\mathbf{1}$, where $\mathbf{1}$ is the second-order identity tensor, and compression is viewed *negative*. Denote the *variable* stress tensor in the composite by $\boldsymbol{\sigma}(x)$, where x is the position vector of a typical point in the composite. When measured relative to the surrounding water pressure p, the average stress of the composite in the absence of any externally applied loads must be zero, i.e., $\int_V \boldsymbol{\sigma}(\boldsymbol{x})\,\boldsymbol{dV} = \mathbf{0}$, where V is the total volume of the composite [Nemat-Nasser and Hori, 1993]. This yields,

$$\bar{\boldsymbol{\sigma}}_M = w\Pi(M^+)\,\mathbf{1} = \phi\frac{2\rho_d RT}{EW}\,\mathbf{1}, \tag{30}$$

where, as before, ρ_d is the dry density and EW is the equivalent weight, and where $\bar{\boldsymbol{\sigma}}_M$ is the stress $\boldsymbol{\sigma}(x)$ averaged over the volume of the matrix material only, i.e., excluding the clusters. Hence, for a fully hydrated composite, the *average* pretension in the backbone polymer matrix due to hydration is hydrostatic tension and independent of the water intake, w (except through the dependency of ϕ on w). Indeed, since the value of EW/ρ_d is independent of the nature of the cations, only the osmotic coefficient ϕ in Eq. (30) depends on the cation and its concentration. For Nafion 1200 with $\phi = 1$, for example, the average pretension is about 8.6 MPa. On the other hand, the *nominal* cross-sectional stress (this is the force carried by the polymer matrix, measured per unit total area of the cross section of the hydrated membrane including the area of the clusters) due to the average stress in the polymer, is a function of the amount of the hydration and hence varies with the cations. By considering a spherical cluster in a cubic unit cell, it is readily shown that this nominal tension (due to the average stress only) may be estimated by

$$t_n = (2\phi\rho_d RT/EW)\left[1-\pi\left(\frac{3}{4\pi}\frac{w}{1+w}\right)^{2/3}\right],$$

where the quantity inside the brackets is the matrix area fraction, i.e., the area of the matrix material divided by the total cross-sectional area; for a discussion of the full stress field, see Sec. 6.5.7.9.

Table 4: Calculated osmotic pressures developed during hydration of bare (Nafion1200) samples. Ion molalities are derived from Gierke [1981]; osmotic coefficients used are for the ideal case ($\phi = 1$).

Ion	**H^+**	**Li^+**	**Na^+**	**K^+**	**Rb^+**	**Cs^+**
ρ_{dry}	2.075	2.078	2.113	2.141	2.221	2.304
EquivalentWeight, EW	1200	1206	1222	1238	1284	1332
Water Content, *w*	0.697	0.617	0.443	0.187	0.179	0.136
1 L 'dry' Nafion 1200 upon hydration contains:						
n(H_2O), moles	38.72	34.28	24.61	10.39	9.94	7.56
n(ion), moles	1.73	1.72	1.73	1.73	1.73	1.73
ions per water	0.04	0.05	0.07	0.17	0.17	0.23
x(H_2O)	0.92	0.91	0.88	0.75	0.74	0.69
x(ion)	0.08	0.09	0.12	0.25	0.26	0.31
ν m(ion) molality	4.96	5.59	7.81	18.49	19.32	25.44
Π (MPa), Osmotic Pr.	12.35	13.91	19.44	46.05	48.11	63.34

6.5.4 Basic Model Assumptions

Consider a model in which the anions are permanently attached to the fluorocarbon backbone, while the countercations are free to move through the water-saturated interstitial regions. Under the action of an electric potential applied to the electrodes of an IPMC, the cations are redistributed, resulting in a microscopic, *locally* imbalanced net charge density that produces internal stresses acting on the backbone polymer. The redistribution of the charges is generally accompanied by changes in the volume of the clusters caused by the electrostatic, osmotic, and elastic interaction forces that develop within and outside the clusters. The change in the cluster volume is accompanied by the commensurate change in its water content, as well as in relaxation or further stretching of the polymer chains between the clusters.

In general, all of these effects (i.e., electrostatic, osmotic, and elastic) are significant in producing the initial fast response of the IPMC, depending on the cation. Models are proposed which emphasize various possible effects in describing the IPMC's initial fast motion. The *hydraulic model* asserts that ions

in solution are hydrated to a greater or lesser extent, and the ions migrating within IPMC materials carry water molecules whose bulk contributes to volumetric swelling stresses within the membrane. The *electrostatic model* asserts that the locally imbalanced net charge density produces internal stresses acting on the backbone polymer, relaxing the polymer chains in the anion-rich regions and further extending them in the cation-rich regions. This model is thus based on the observation by Forsman that the clustering of ionic groups in sulfonate ionomers is accompanied by an increase in the mean length of the polymer chains [Forsman, 1982]. This prestretching of the polymer is in addition to the hydration-induced pretension discussed earlier. The *hybrid model* asserts that all the electrostatic, osmotic, and elastic effects are important, although one or the other may dominate, depending on the case considered, and that water (or other solvents) migration in and out of the clusters *is a response to rather than the cause of the cluster swelling*.

For the slow relaxation motion, it appears that the electro-osmotic forces, as well as the change in the polymer stiffness, play important roles, and that *the reorganization of cations within the cation-rich clusters is the most significant controlling factor*. It is expected that viscous effects would mediate the flow of water during ion migration via electro-osmosis. Solute concentration and matrix stiffness strongly influence the magnitude of electro-osmotic flow. Ions migrating through inhomogeneous structures may exhibit a *solvation number* (SN) smaller than the bulk, owing to the tortuous route through which the ion must travel.

6.5.5 Hydraulic Model

Hydraulic models for IPMC actuation assume that water migration between ionomer clusters causes differential swelling, yielding bending actuation. The mechanism of water migration has been attributed to primary and secondary hydraulic motions. Applied voltages cause migration of ionic species, and the primary hydraulic effect is assigned to the motion of water molecules that are closely associated to ions by solvation. The secondary hydraulic effect includes forces that derive from the initial migration of ions—electro-osmotic effects.

6.5.5.1 Primary Hydraulic Effects

Ions in aqueous environments are closely associated with water molecules (*solvation water*). It has been proposed that the migration of ions through IPMC materials involves the concomitant migration of water, either through solvation water or electro-osmotic migration. According to this model, the increase in cluster volume caused by water migration is sufficient to cause volumetric strain within the IPMC matrix, yielding the observed bending strain in the material and actuation towards the anode. As pointed out before, experimental observations do

not support the basic assumptions of this model, as further discussed in the sequel.

The instantaneous contact of water molecules with an ion is a *static* description of the ion's local environment. This is known as the ion's *coordination number* (CN) or the *secondary hydration number* (SN). Ion CN is determined from small-angle x-ray and neutron diffraction studies.

Under dynamic conditions, ions in aqueous environments are not freely moving species. Instead, ions are solvated by a shell of strongly interacting water molecules known as water of solvation, or *primary hydration water*. The SN is a dynamic value, representing the number of water molecules that migrate with ions during diffusion and motion. Generally, water molecules that remain in association with the ion for longer periods than the diffusive lifetime (τ) are considered solvation waters. Ion SNs are derived from ultrasonic vibration potentials [Zana and Yeager, 1966]. Solvation numbers may be deduced from the apparent molar volume of an ion, as derived from the electro-osmotic flow of water between two electrodes. Strong local electric fields surrounding an ion have the effect of compressing the volume of surrounding waters. As a result, the apparent molar volume is not a direct representation of the absolute solvation number of an ion.

Protons provide an interesting exception to this case, as the proton has a large number of tightly held secondary waters of hydration, as pointed out before. Its motion through the water, though, does not include these hydration waters. Its migration is not by diffusion, but rather by a *hopping* mechanism that is an order of magnitude faster than diffusion—the *Grotthuss mechanism* [Agmon, 1995, 1999]. In this event, H^+ does not transport any water with it, and the process is so fast that no significant diffusion can accompany it. As discussed in Sec. 6.5.1, *the cluster volume actually increases with proton depletion and decreases with excess proton concentration*. The hydraulic model without inclusion of other effects cannot account for the resulting motion of the associated IPMC, which is principally similar to that of other metallic cation composites. Furthermore, the hydraulic model does not have any convincing explanation for the observed large back relaxation (see Fig. 13) that occurs under a suddenly applied and sustained step voltage (dc). As mentioned already, *through a slow voltage buildup, a slow bending towards the cathode only (i.e., without any preceding bending towards the anode) can be produced, contradicting the hydraulic model*. We thus conclude that the hydraulic model does not have any basis in experiments and should be abandoned.

6.5.6 Hybrid Models

We expect models that incorporate each effect to prove the most useful. The scale of each effect must be determined, as well as the time-scale contribution of each term to the overall displacement of IPMC materials (cf. dc actuation). Each effect may be investigated by variations of known material parameters such as ion charge, radius, and solvation (i.e., hydration); solvent viscosity and dielectric

constant; ion "hydrophobicity" or "hydrophilicity"; and polymer-matrix cluster size, equivalent weight, branch length, and end group anion species. Correlation between mechanical and micromechanical observables and molecular interactions will prove the most useful in improving the force yield of IPMC materials. Nemat-Nasser [2002] proposes a model that incorporates electrostatic, osmotic, and elastic effects in the actuation of IPMCs, and leads to results in good accord with experiments, including initial fast motion, subsequent back relaxation, and the response upon shorting. Various essential features of this model are summarized in what follows.

6.5.7 Basic Equation of Hybrid Model

The basic field equations, which include the electrostatic and the osmotic effects, are now summarized and discussed. To be specific, the solvent is assumed to be water, with actuation occurring in an aqueous environment.

6.5.7.1 Electrostatic and Transport Equations

The distribution of cations under the action of an imposed electric potential must first be established. With D, E, and φ, respectively denoting the electric displacement, the electric field, and the electric potential, the charge distribution is governed by the following field equations:

$$\frac{\partial D}{\partial x} = \rho\,,\ D = \kappa_e E\,,\ E = -\frac{\partial \varphi}{\partial x}\,,\ \rho = (C^+ - C^-)F\,, \tag{31}$$

where only the one-dimensional case is considered, with x measuring length along the cross section; ρ is the charge density (C/m^3), C^+ and C^- are the positive and negative ion densities (mol/m^3), respectively, F is Faraday's constant (96,487 C/mol), and κ_e is the effective electric permittivity of the polymer. The distribution of the counter-ions and the associated solvent molecules are governed by coupled continuity equations,

$$\frac{\partial}{\partial t}\ln(1+w) + \frac{\partial v}{\partial x} = 0, \quad \frac{\partial C^+}{\partial t} + \frac{\partial J^+}{\partial x} = 0, \tag{32}$$

where $v = v(x, t)$ is water velocity (flux) and $J^+ = J^+(x,t)$ is the cation flux, both in the thickness (i.e., x) direction. These fluxes are usually expressed as linear functions of the gradients $\partial\mu^w/\partial x$ and $\partial\mu^+/\partial x$ (i.e., forces), through empirical coefficients. The electro-chemical potentials of the solvent (water, here) and the cations are given by

$$\mu^w = \mu_0^w + 18(10^{-6}\, p - 10^{-3} RT\phi\nu m),\ \mu^+ = \mu_0^+ + RT\ln(\gamma^+ C^+) + F\varphi, \qquad (33)$$

where the first term on the right side of these equations include the reference and the normalizing values of the associated potential; see also comments after expression (29).

As noted before, some water molecules are carried by hydrophilic cations (except for H^+). If SN is the *dynamic solvation number*, i.e., mole water molecules actually transported per mole migrating cations, the resulting volumetric strain then would be

$$\varepsilon_v^* = 18\times 10^{-6}(C^+ - C^-)SN. \qquad (34)$$

However, recent current-flow measurements (Nemat-Nasser and Wu, 2003a) show continued cation addition to the cathode clusters while these clusters are actually in contact with each other (Nafion-based IPMCs in alkali cation forms), suggesting that the cations rather than their solvation water molecules are of primary importance in the IPMC actuation. Therefore, in what follows, SN is set equal to zero, and the volume strain is calculated directly by considering cation transport and the resulting forces that affect the volume of the clusters, driving water into or out of the clusters.

6.5.7.2 Estimate of Length and Time Scales

Consider now the problem of cation redistribution and the *resulting induced* water diffusion. The diffusion-controlled water migration is generally a slow process. Thus, only the second continuity equation in Eq. (32) is expected to be of importance in describing the initial cation redistribution, while the first continuity equation applies to the subsequent resulting water diffusion. The corresponding cation flux can be expressed as

$$J^+ = -\frac{D^{++}C^+}{RT}\frac{\partial \mu^+}{\partial x} + \frac{D^{+w}C^+}{RT}\frac{\partial \mu^w}{\partial x}, \qquad (35)$$

where D^{++} and D^{+w} are empirical coefficients. It is very difficult to estimate or measure these coefficients in the present case. Therefore, instead, use the well-known Nernst equation [Lakshminarayanaiah, 1969],

$$J^+ = -D^+\left(\frac{\partial C^+}{\partial x} + \frac{C^+F}{RT}\frac{\partial \varphi}{\partial x} + \frac{C^+V^{+w}}{RT}\frac{\partial p}{\partial x}\right) + C^+ v, \qquad (36)$$

with D^+ being the ionic diffusivity coefficient. Upon linearization, obtain [Nemat-Nasser and Li, 2000; and Nemat-Nasser and Thomas, 2001],

$$\frac{\partial}{\partial x}\left[\frac{\partial(\kappa E)}{\partial t} - D^{+}\left(\frac{\partial^{2}(\kappa E)}{\partial x^{2}} - \frac{C^{-}F^{2}}{\kappa RT}(\kappa E)\right)\right] = 0. \tag{37}$$

This equation includes a natural length scale, ℓ, and a natural time scale, τ, respectively characterizing the length of the boundary layers and the relative speed of cation redistribution,

$$\mathrm{l} = \left(\frac{\bar{\kappa}RT}{C^{-}F^{2}}\right)^{1/2}, \quad \tau = \frac{\mathrm{l}^{2}}{D^{+}}, \tag{38}$$

where $\bar{\kappa}$ is the overall electric permittivity of the hydrated IPMC strip, which can be estimated from its measured capacitance (if *Cap* is the measured overall capacitance, then $\bar{\kappa} = 2HCap$). Therefore, l can be estimated directly from Eq. $(38)_1$, whereas the estimate of τ will require an estimate for D^{+}. It turns out that the capacitance of the Nafion-based IPMCs (about 200- to 225-μm thick) that have been examined in the first author's laboratories ranges from 1 to 60 mF/cm^2, depending on the sample and the cation form. This suggests that ℓ may be 0.5 to 6 μm, for the Nafion-based IPMCs. Thus, ℓ^2 is of the order of 10^{-12} m^2, and for the relaxation time τ to be of the order of seconds, D^{+} must be of the order of 10^{-12} m^2/s. Our most recent experimental results (Nemat-Nasser and Wu, 2003a) suggest this to be the case. Indeed, direct measurement of current flow through Nafion-based IPMC strips under a constant voltage shows $\tau = O(1)$ s in an aqueous environment. Since ℓ is linear in $\sqrt{\kappa}$ and $\bar{\kappa}$ is proportional to the capacitance, it follows that ℓ is proportional to the square root of the capacitance.

6.5.7.3 Equilibrium Solution

To calculate the ion redistribution caused by the application of a step voltage across the faces of a hydrated strip of IPMC, first examine the time-independent *equilibrium* case with J^{+}= 0. In the cation-depleted (anode) boundary layer the charge density is $-C^{-}F$, whereas in the remaining part of the membrane the charge density is $(C^{+} - C^{-})F$. Let the thickness of the cation-depleted zone be denoted by ℓ', and set

$$Q(x,t) = \frac{C^{+} - C^{-}}{C^{-}}, \quad Q_{0}(x) = \lim_{t\to\infty} Q(x,t). \tag{39}$$

Then, it can be shown that [Nemat-Nasser, 2002] the equilibrium distribution is given by

$$Q_0(x) \equiv \begin{cases} -1 & \ldots \text{for } x \le -h + \ell' \\ \dfrac{F}{RT}[B_0 \exp(x/\ell) - B_1 \exp(-x/\ell)] , & \\ & \ldots \text{for } -h + \ell' < x < h \end{cases} \tag{40}$$

where the following notation is used:

$$B_1 = K_0 \exp(-a'), \quad \frac{\ell'}{\ell} = \sqrt{\frac{2\phi_0 F}{RT}} - 2, \quad B_2 = \frac{\phi_0}{2} - \frac{1}{2} K_0 \left[\left(\frac{\ell'}{\ell} + 1 \right)^2 + 1 \right],$$

$$B_0 = \exp(-a)\left[\phi_0 / 2 + B_1 \exp(-a) + B_2 \right], \quad K_0 = \frac{F}{RT}, \tag{41}$$

ϕ_0 is the applied potential, $a \equiv h/\ell$, and $a' \equiv (h - \ell')/\ell$. Since ℓ is only 0.5 to 3 μm, $a \equiv h/\ell$, $a' \equiv h'/\ell) >> 1$, and hence $\exp(-a) \approx 0$ and $\exp(-a') \approx 0$. The constants B_0 and B_1 are very small, of the order of 10^{-17} or even smaller, depending on the value of the capacitance. Therefore, the approximation used to arrive at Eq. (40) does not compromise the accuracy of the results. Remarkably, the estimated length of the anode boundary layer with constant negative charge density of $-C^- F$, i.e., $\ell' = \left(\sqrt{2\phi_0 F / RT} - 2 \right) \ell$, depends only on the applied potential and the characteristic length ℓ. For $\phi_0 = 1\,\text{V}$, for example, $\ell' \approx 6.8\ell$.

6.5.7.4 Temporal Variation of Cation Distribution

Since $a = h/\ell \approx 50$, it can be shown that

$$Q(x,t) \approx g(t) Q_0(x), \quad g(t) = 1 - \exp(-t/\tau). \tag{42}$$

Thus, the spatial variation of the charge distribution can be separately analyzed and then modified to include the temporal effects.

6.5.7.5 Clusters in Anode Boundary Layer

Consider the anode boundary layer, and note from

$$\int_{-h'}^{0} Q_0(x) dx = \ell \tag{43}$$

that the *effective* total length of the anode boundary layer, L_A, can be taken as

$$L_A \equiv \ell' + \ell = \left(\sqrt{\frac{2\phi_0 F}{RT}} - 1 \right) \ell. \tag{44}$$

Thus, the equilibrium charge density is $Q_0(x) = -1$, in $-h \le x < -h + L_A$, and zero in $-h + L_A \le x < 0$. In the anode boundary layer, $-h \le x < -h + L_A$, the cation density is $C^+ = C^- \exp(-t/\tau)$ and the total ion (cation and anion) concentration is $C^- + C^+ = C^-[2 - g(t)]$. These expressions are then used to estimate the osmotic pressure, $\Pi_A(t)$, the effective electric permittivity, $\kappa_A(t)$, and the electrostatic forces within the anode boundary layer. The details are found in Nemat-Nasser [2002]. The electrostatic effects include anion-anion interaction, $p_{AA}(t)$, and dipole-dipole interaction, $p_{ADD}(t)$, forces. The former increases in time while the latter decreases as cations migrate out of the anode boundary layer. The decrease in ion concentration reduces the osmotic pressure, increases the dielectric parameter, both of which tend to decrease the average cluster size in this zone, contributing to the initial bending towards the anode. This also shows that the back relaxation must necessarily be the result of cation activity in the cathode boundary layer, as discussed below. Finally, the resulting pressure within a typical cluster in the anode boundary layer then becomes

$$\begin{aligned}
&t_A = \Pi_A(M^+, t) + p_{AA}(t) + p_{ADD}(t) + \sigma_r(a_0, t), \\
&\Pi_A(t) = \frac{\phi Q_B^- K_0}{w_A(t)}[2 - g(t)], \quad Q_B^- = \frac{\rho_B F}{E W_{ion}}, \\
&p_{AA}(t) = \frac{g(t)}{18\kappa_A(t)} Q_B^{-2} \frac{R_0^2}{[w_A(t)]^{4/3}}, \\
&p_{ADD}(t) = \frac{1 - g(t)}{3\kappa_A(t)} Q_B^{-2} \frac{\pm[\alpha_A(t)]^2}{[w_A(t)]^2}, \\
&\sigma_r(a_0, t) = -p_0(t) + K(t)(w_A(t)/w_0)^{-4/3},
\end{aligned} \tag{45}$$

where the last term in Eq. $(45)_1$ is the elastic resistance of the backbone polymer, R_0 is the dry cluster size, and other terms have been defined before; see Nemat-Nasser [2002] for further comments. As shown, all interaction forces are calculated using the corresponding time-dependent water uptake, $w_A(t)$. This water uptake is computed incrementally, using the diffusion equation and the initial and boundary conditions. Since the boundary layer is rather thin, assume uniform w_A and t_A in the boundary layer, and replace the diffusion equation with

$$\frac{\dot{w}_A}{1+w_A} = D_{H_2O}\frac{t_A}{(L_A/2)^2} = D_A t_A, \tag{46}$$

where D_{H_2O} is the hydraulic permeability coefficient. Note that coefficient D_A here includes the effect of the thickness of the boundary layer. We assume that D_A is constant.

6.5.7.6 Clusters in the Cathode Boundary Layer

Consider now the clusters within the *cathode boundary layer*. Unlike in the anode boundary layer, the ion concentration in the cathode boundary layer is sharply variable, and we have

$$\nu_C(x,t) = 2 + Q(x,t) = 2 + \frac{B_0}{K_0}\exp(x/\ell)g(t), \tag{47}$$

based on which the osmotic pressure and dielectric parameter must be computed. In this boundary layer, there are two forms of electrostatic interaction forces. One is repulsion due to the cation-anion pseudo-dipoles already present in the clusters, and the other is due to the extra cations that migrate into the clusters and interact with the existing pseudo-dipoles. The additional stresses produced by this latter effect may tend to expand or contract the clusters, depending on the distribution of cations relative to the fixed anions. Each effect may be modeled separately, although in actuality they are coupled. The dipole-dipole interaction pressure in the clusters may be estimated as

$$p_{CDD}(x,t) = \frac{Q_B^{-2}}{3\kappa_C(x,t)}\frac{\pm[\alpha_C(x,t)]^2}{[w_C(x,t)]^2}[1-g(t)], \tag{48}$$

where the subscript C denotes the corresponding quantity in the cathode boundary layer; $\alpha_C(x,t)$ is the dipole arm that can evolve in time, as the cations reconfigure under the action of the strong sulfonates (but not necessarily under the action of the weak carboxylates). We represent the interaction between the pre-existing dipoles and the additional cations that move into a cluster under the action of an applied voltage, by dipole-cation interaction stresses defined by

$$p_{DC}(x,t) = \frac{2Q_B^{-2}}{9\kappa_C(x,t)}\frac{a_C(x,t)\alpha_C(x,t)}{[w_C(x,t)]^2}g(t) \approx \frac{2Q_B^{-2}}{9\kappa_C(x,t)}\frac{R_0\alpha_C(x,t)}{[w_C(x,t)]^{5/3}}g(t). \tag{49}$$

This equation is obtained by placing the extra cations at the center of a sphere of (current) radius $a_C(x,t)$, which contains uniformly distributed radial dipoles-of-moment arm $\alpha_C(x,t)$ on its surface, and then multiplying the result by $g(t) = 1 - \exp(-t/\tau)$.

6.5.7.7 Reverse Relaxation of IPMC under Sustained Voltage

For sulfonates in a Nafion-based IPMC, extensive restructuring and redistribution of the extra cations, appear to underpin the observed reverse relaxation of the Nafion-based IPMC strip. To represent this, modify Eq. (49) by a *relaxation factor*,

$$\begin{aligned} p_{DC}(x,t) &\approx \frac{2Q_B^{-2}}{9\kappa_C(x,t)} \frac{R_0 \alpha_C(x,t)}{[w_C(x,t)]^{5/3}} g(t) g_1(t), \\ g_1(t) &= [r_0 + (1-r_0)\exp(-t/\tau_1)], \quad r_0 < 1, \end{aligned} \tag{50}$$

where τ_1 is the relaxation time, and r_0 is the equilibrium fraction of the dipole-cation interaction forces.

The total stress in clusters within the cathode boundary layer is now approximated by

$$t_C = \sigma_r(a_0,t) + \Pi_C(x,t) + p_{CDD}(x,t) + p_{DC}(x,t). \tag{51}$$

The rate of change of water uptake in the cathode boundary layer is governed by the diffusion equation,

$$\frac{\dot{w}_C}{1+w_C} = D_{H_2O} \frac{\partial^2 t_C}{\partial x^2}, \tag{52}$$

subject to the boundary and initial conditions

$$\begin{aligned} &t_C(h,t) = 0, \quad w_C(0,t) = w_0, \quad t > 0, \\ &w_C(x,0) = w_0, \quad 0 < x < h, \end{aligned} \tag{53}$$

where w_0 is the uniform water uptake just prior to the cation redistribution. This is a nonlinear initial-boundary value problem, whose complete solution would require a numerical approach. To reveal the essential micro-mechanisms of the actuation, use the thinness of the cathode boundary layer and replace the spatial gradients by the corresponding difference expression, to obtain an average value of the water uptake in this boundary layer.

The overall charge neutrality requires that

$$\int_0^h Q(x,t)dx = L_A g(t). \tag{54}$$

Define an *effective* length and ion density for an equivalent cathode boundary layer of uniform cation distribution, respectively by

$$L_C = 2\left(h - \frac{1}{L_A}\int_0^h xQ_0(x)dx\right), \quad \bar{\nu}_C = 2 + \frac{L_A}{L_C}g(t), \tag{55}$$

and calculate the osmotic pressure and all other quantities using this *equivalent* boundary layer with *uniform ion and water distribution.* In particular, the average water uptake, $\bar{w}_C(t)$, is obtained using

$$\frac{\dot{w}_C}{1+w_C} = D_C\bar{t}_C, \quad \bar{t}_C(t) = \bar{\sigma}_r(a_0,t) + \bar{\Pi}_C(t) + \bar{p}_{CDD}(t) + \bar{p}_{DC}(t), \tag{56}$$

where the barred quantities denote the average values. The anode and the equivalent cathode boundary layer thicknesses are related by $D_C = (L_A/L_C)^2 D_A$.

6.5.7.8 Tip Displacement

The tip displacement of the cantilever is now calculated incrementally, using the rate version of Eqs. (22) and (23), which can be expressed as

$$\frac{\dot{u}}{L} = \frac{LY_{BL}}{4H^3(3\bar{Y}_{\mathrm{IPMC}} - 2Y_B)}\int_{-h}^{h} x\frac{\dot{w}(x,t)}{1+w(x,t)}dx. \tag{57}$$

For the equivalent uniform boundary layers, the integral in the right-hand side of this equation can be computed in closed form, yielding

$$\frac{\dot{u}}{L} = \frac{Y_{BL}}{(3\bar{Y}_{\mathrm{IPMC}} - 2Y_B)}\frac{hL}{4H^2}\left(\frac{\dot{w}_A}{1+w_A}\frac{L_A}{H} - \frac{\dot{w}_C}{1+w_C}\frac{L_C}{H}\right), \tag{58}$$

where we have neglected terms of the order of $O(L_A/H)^2$. Combining this with Eqs. (46) and (56), we now have

$$\frac{\dot{u}}{L} = \frac{Y_{BL}}{(3\bar{Y}_{\text{IPMC}} - 2Y_B)} \frac{hLL_A}{4H^3} D_A \left(t_A - \bar{t}_C \frac{L_A}{L_C} \right), \tag{59}$$

where t_A and $\bar{t}_C$ are given by Eqs. (51) and (56), respectively. This equation may now be integrated incrementally.

6.5.7.9 Estimate of κ_e for Hydrated Nafion

Using a double inclusion model, Nemat-Nasser and Li [2000] show that the effective electric permittivity of the membrane can be evaluated as

$$\kappa_e = \frac{\kappa_p + \kappa_w + c_w(\kappa_p - \kappa_w)}{\kappa_p + \kappa_w - c_w(\kappa_p - \kappa_w)} \kappa_p, \tag{60}$$

where the subscripts p and w refer to the electric permittivity of water (solvent) and polymer, respectively. This expression has been used to obtain the estimate of Eq. (14) as well as Eq. (16).

6.5.7.10 Example of Actuation

To check whether or not the proposed model captures the essential features of the observed actuation response of the Nafion-based IPMCs, consider a cantilevered strip of fully hydrated IPMC in Na^+-form. Figure 15 shows (geometric symbols) the measured tip displacement of a 15mm long cantilever strip that is actuated by applying a 1.5V step potential across its faces, maintaining the voltage for about 32 seconds and then removing the voltage while the two faces are shorted. The initial water uptake is $w_{\text{IPMC}} = 0.46$, and the volume fraction of metal plating is 0.0625. Hence, the initial volume fraction of water in the Nafion part of the IPMC is given by $w_0 = w_{\text{IPMC}}/(1 - f_M) = 0.49$. The formula weight of sodium is 23, and the dry density of the bare membrane is 2.02g/cm^3. The equivalent weight for the bare Nafion (and *not* the IPMC) then becomes EW_{Na^+} = 1122 g/mol. The initial value of C^- for the bare Nafion then becomes

$$C^- = 10^6 \frac{\rho_B}{EW_{Na^+}(1 + w_0)} = 1,208 \,\text{mol/m}^3.$$

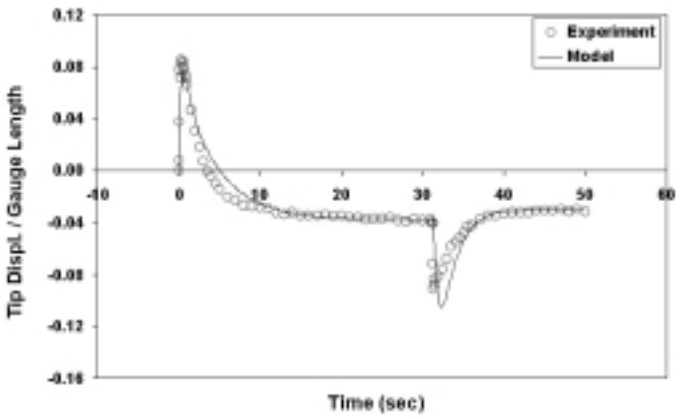

Figure 15: Tip displacement of a 15mm cantilevered strip of a Nafion-based IPMC in Na^+-form, subjected to 1.5 V step potential for about 32 seconds, then shorted; the heavy solid curve is the model and the geometric symbols are experimental points.

The thickness of the hydrated strip is measured to be $2H = 224\mu m$, and based on inspection of the microstructure of the electrodes, set $2h \approx 212\mu m$. The effective length of the anode boundary layer for $\phi_0 = 1.5\,V$ is $L_A = 9.78l$, from Eq. (55) the thickness of the equivalent uniform cathode boundary layer becomes $L_C = 2.84l$, and $l = 0.862\mu m$ for $\phi_0 = 1.5$ V. The electric permittivity and the dipole length are calculated using $a_1 = 1.5234\times10^{-20}$ and $a_2 = -0.0703\times10^{-20}$. The measured capacitance ranges from 10 to 20 mF/cm^2, and we use Cap = 15 mF/cm^2.

The measured stiffness of bare Nafion and the corresponding IPMC in Na-form are shown in Fig. 16, as function of the hydration, for loading and unloading. The solid curves are the corresponding model predictions, calculated using expression (12), with the following values of the parameters: n_0 = 0.01, ϕ = 1, CN = 4.5. Other actuation-model parameters are: $D_A = 10^{-2}$ (when pressure is measured in MPa), $\tau = 1/4$ and $\tau_1 = 4$ (both in seconds), SN = 0, and $r_0 = 0.25$. In line with the observation that the cations continue to move into the cathode boundary layer long after the back relaxation has started, we have set SN = 0. Since $w_0 \approx (a/R_0)^3$, where a is the cluster size at water uptake w_0, we have set $R_0 \approx w_0^{-1/3} a$, and adjust a to fit the experimental data; here, a = 1.65 nm, or an average cluster size of 3.3 nm, prior to the application of the potential. The fraction of cations that are left after shorting is adjusted to $r = 0.03$.

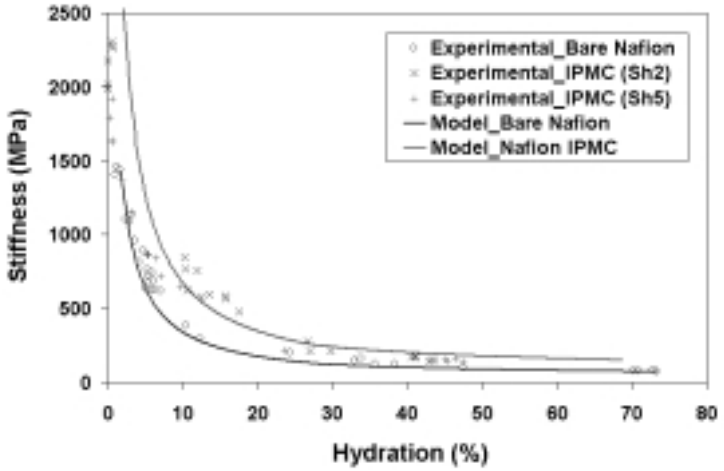

Figure 16: Uniaxial stiffness (Young's modulus) of bare Nafion 117 (lower data points and the solid curve, model) and an IPMC (upper data points and light curve) in the Na+-form versus hydration water.

The solid line in Fig. 15 shows the model result. While the values of the parameters that are used are reasonable, they are chosen to give good comparison with specific experimental data. These data are from one test only. The variation of the response from sample to sample, or even for the same sample tested at various times, is often so great that only a qualitative correspondence between the theoretical predictions and the experimental result in general can be expected, or reasonably required. In examining the influence of various competing factors, it has become clear that the electrostatic forces are most dominant, as has also been observed by Nemat-Nasser and Li (2000) who used a different approach. Although the osmotic effects are also relevant, they have less impact in defining the initial actuation and subsequent relaxation of the Nafion-based IPMCs.

6.5.7.11 Hydrated IPMC Strip as Sensor

Assume the IPMC strip is suddenly bent. An electric potential will be generated across the composite. Nemat-Nasser and Li [2000] assume that this is due to the differential displacement of the effective centers of the anions and cations within each cluster, producing an effective dipole. Since this differential displacement is less than second-order in magnitude, the resulting electric potential will also be of the same order of magnitude. The displacement along the *x*-axis of the membrane subjected to an applied bending curvature is given by Love [1944]:

$$u = (z^2 + \nu x^2 - \nu y^2)/2R_c\,, \tag{61}$$

where ν is the Poisson ratio of the membrane, and R_c is the imposed radius of curvature. This imposed displacement field distorts the ionic clusters, creating an effective dipole within each cluster. To estimate the value of this dipole, consider a spherical cluster of radius r_c, with the center at (x_α, 0, 0). Assume that the fixed anions are uniformly distributed on the surface of this sphere, while the cations are uniformly distributed over a sphere of the same center but of radius r_c - r_i, where r_i is the distance between the anion and cation in an ion pair [see Fig. 17(a)].

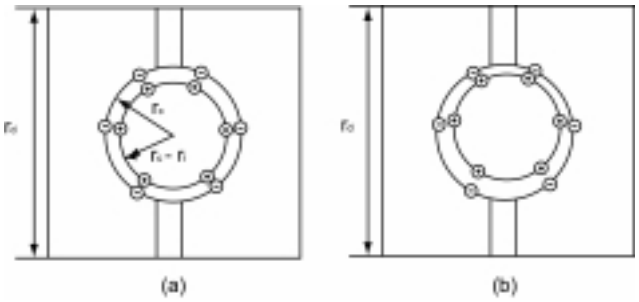

Figure 17: Schematic representation of IPMC clusters: (a) an arrangement of ions into dipoles within cluster, and (b) a dipole induced by imposed bending curvature.

The distributed charges are equivalent to an effective total charge located at the common center of the two spheres prior to the applied distortion, producing zero total charge and dipole. The imposed deformation displaces the effective anion and cation charge centers by different amounts, producing an effective dipole [see Fig. 17(b)]. The displacement of the effective charge center is estimated by averaging the resulting surface displacement over each surface. The separation of the effective centers of anions and cations in a cluster, due to the imposed bending curvature, denoted by $\Delta d(x_\alpha)$ for the α-th cluster, is then given by

$$\Delta d(x_\alpha) = [r_c^2 - (r_c - r_i)^2]/6R_c \approx r_c r_i / 3R_c , \qquad (62)$$

which is independent of x_α. The separation of the effective charge centers introduces a dipole $\boldsymbol{\mu}$ in the cluster, which induces a potential field. The magnitudes of the dipole, μ, and the resulting potential, ϕ_α, are given by

$$\mu(x_\alpha) = q_{total}\Delta d = C^- F r_d^3 r_c r_i / 3R_c , \ \phi_\alpha = (q_{total} r^2 + \boldsymbol{\mu} \cdot \boldsymbol{r})/(4\pi\kappa_w r^3), \qquad (63)$$

where q_{total} is the total positive charge inside the cluster, $\boldsymbol{r}$ is the position vector of magnitude r with respect to the induced dipole, and κ_w is the electric permittivity of water ($78\kappa_0$). Now we have a series of clusters of water

embedded in the polymer backbone, each with a dipole at its center. The electric field in the polymer, induced by the dipole located at the cluster center, is given by

$$E = 12\sum_{n=0}^{n=\infty} \mu / [(2n+1)^3 4\pi\kappa_w (2\kappa_p / \kappa_w + 1)(r_d / 2)^3], \tag{64}$$

where E is the magnitude of the resulting electric field. This leads to a potential difference across the thickness, given by

$$\Delta\varphi = 2hE\,. \tag{65}$$

For reasonable estimates of the parameters, this equation yields potential values of tens of mV for a sudden deformation of an IPMC. Figure 17, from Nemat-Nasser and Li [2000], illustrates this.

6.6 Development of IPMC Applications

6.6.1 Proposed Applications

The ultimate success of IPMC materials depends on whether or not suitable applications can be found. Whereas IPMC materials cannot offer the force output (of some materials) or the driving frequency (of others), a large number of applications have been proposed which take advantage of IPMCs' bending actuation, low voltage/power requirements, small and compact design, lack of moving parts, and relative insensitivity to damage. In this section, a number of suggested and prototype applications are described. As well, applications of IPMC materials are presented elsewhere within this book (Oguro, Chapter 13).

Osada and colleagues have described many applications for IPMCs, including catheters [Sewa et al., 1998; Oguro et al., 1999], elliptic friction drive elements [Tadokoro et al., 1997], and ratchet-and pawl-based motile species [Osada et al., 1992]. IPMCs have been suggested in applications to mimic biological muscles; Caldwell has investigated artificial muscle actuators [Caldwell, 1990; Caldwell and Tsagarakis, 2000], and Shahinpoor has suggested applications ranging from peristaltic pumps [Segalman et al., 1992] and devices for augmenting human muscles [Shahinpoor, 1996], to robotic fish [Shahinpoor, 1992]. These materials have been suggested for use as fabrics for use in theatrical costuming and special effects (A. Lauer, Alley Theater, Houston, TX, personal communication).

Bar-Cohen and others have discussed the use of IPMC actuators in space-based applications [Bar-Cohen et al., 1998, 1999a], as their lack of multiple moving parts is ideal for any environment where maintenance is difficult. As described above, IPMCs offer application in vibration sensing applications [Sadeghipour et al., 1992]. Besides these novel applications, IPMCs find

applications in other disciplines, including fuel cell membranes, electrochemical sensing [DeWulf and Bard, 1988], and electrosynthesis [Potente, 1988]. Much of the interest in these materials has stemmed from these already established applications for Nafion-type materials. The commercial availability of Nafion has allowed significant opportunity to find alternate uses for these materials. Growth and maturity in the field of IPMC actuators will require exploration beyond these commercially available polymer membranes, as the applications for which they have been designed are not necessarily optimal for IPMC actuators.

6.7 Discussion: Advantages/Disadvantages

6.7.1 Force Generation

IPMC materials do not offer an appreciable power output (estimated at 10 W/kg [Wax and Sands, 1999]), as compared with natural muscle (1000 W/kg), pneumatic, piezoelectric, or hydraulic components. Indeed, it must be recognized that each method of force generation may prove optimal in specific applications. IPMC materials will show similar niche applications based on those properties unique to IPMC actuators. Some of these properties are addressed below.

6.7.2 Low Power Requirements

Unlike other EAP materials [Pelrine et al., 2000], IPMC materials can actuate under applied potentials as low as 1 V. Larger displacements can be obtained using larger voltages, but operation at voltages above 1.23 V is prohibitive due to concomitant electrolysis of water. The electrolytic breakdown of water significantly increases the operating currents required for IPMC actuators, and the production of oxygen and hydrogen gases can contaminate an operating platform. Nonplatinum electrodes, on the other hand, are more easily polarized and develop an overpotential that increases the voltage required for water electrolysis. Usually this is disadvantageous for efficient electrolysis, but Oguro has taken advantage of this phenomenon by creating IPMCs containing all-gold electrodes that can be driven at 2.0 V without a noticeable increase in current or gas evolution [Oguro et al., 1999].

6.7.3 Hydration Requirements

IPMC materials require the presence of water for operation. Without water as a solvent, migration of cation species is curtailed, reducing or eliminating power output. Strategies that seek to contain water within the IPMC must adhere strictly to the 1.23-V electrolysis limit, as the splitting of water has the effect of dehydrating each sample.

Nafion ionomers are compatible with a large number of solvents having higher electrolytic voltages. This would allow operation above the 1.23-V limit

for water. Unfortunately, it is expected that the lower conductivity of these organic solvents will have a detrimental effect on IPMCs' overall force generation.

6.7.4 Sample Contamination

Due to the equilibrium nature of ion exchange in ionomeric polymers, care must be taken to prevent sample contamination when IPMCs are operated in the presence of any competing cationic species (such as salt water). For example, a sample prepared in the lithium form will rapidly exchange with sodium ions if available. Since power output in sodium IPMCs is less than in lithium samples, sample composition is an important parameter that must be considered. Simply handling IPMCs in the lithium form with one's bare hands is sufficient to contaminate the sample with sodium ions. It is recommended that all IPMC materials be handled using clean forceps or protective gloves. Treatment of prepared samples with a cladding layer to prevent further ion exchange has been proposed, but protective strategies used have not been sufficient to prevent ion contamination in IPMC materials.

Regardless of an IPMC's ion exchange equilibrium constant [Steck and Yeager, 1980; Cwirko and Carbonell, 1992], it must be realized that ion exchange is a statistical process. One piece of sodium-form IPMC in a solution of lithium electrolyte will experience ion exchange, given enough time and a large enough reservoir of electrolyte solution. This may limit the use of IPMC actuators in open environments (seawater, blood, or beneath the surface of Europa).

6.7.5 Manufacturing Cost

Current methods for IPMC manufacture rely on expensive noble metals (Pt $20/g, Au $10/g) for the plating process. The method of manufacture includes steeping in hot nitric or hydrochloric acids for cleaning and ion exchange—processes that demand use of unreactive noble metals. In addition, use of IPMC materials at potentials greater than 1.23 V can create transient oxygen and hydrogen species that can corrode non-noble metals. It is anticipated that changes in processing and operating conditions may be able to reduce reliance upon these metals.

In addition, IPMC materials have heretofore been manufactured using Nafion perfluorosulfonate membrane materials. Since these materials are somewhat expensive ($8/g), some consideration should be made for alternative matrix materials. Of course, the degree to which IPMC behavior is dependent on the unique properties of perfluorinated sulfonic acid ionomers may limit these opportunities.

6.7.6 Soft Materials—Consistency of Processing

To some degree, IPMC materials suffer from their lack of rigidity. Processing through multiple steps yields materials whose properties may not be consistent from batch to batch. Variations including surface morphology, small bends, ripples, and other processing imperfections can yield large variations in actuator performance. Our solutions to these inconsistencies include working with individual batches and repeating experiments on large numbers of samples. Additionally, our models for force generation anticipate variation in each sample's shape. Bulk processing methods can be addressed after force and power output of IPMC materials are known, and applications are found that justify further optimization of processing conditions.

6.7.7 Bending Mode of Actuation

Description of IPMC materials as "artificial muscles" is problematic, as natural muscles exhibit contractile forces, and IPMC actuation occurs by bending motion. Applications requiring linear actuators may not be ideally suited for IPMC materials; instead, IPMC actuators can find use as positioning actuators or other specialized applications. However, Oguro and colleagues demonstrated several unique applications utilizing bending actuators, including an elliptical friction drive, a ratchet-based crawler, and a two-axis catheter positioner.

IPMC actuators might better be described as plantlike in their motion rather than as animal muscles [Shahinpoor and Thompson, 1995]. Motion in vascular plants is caused by the differential swelling and contraction of waterlogged tissues at either end of a plant's stem. It may prove useful to study the mechanics of plant movement while searching for suitable applications for IPMC actuators.

6.7.8 Scalability

Natural muscles consist of millions of strands of individual muscle fibers. IPMC materials studied to date are large (1–10-mm wide) and are operated as single slabs. A combination of multiple pieces to form IPMC bundles could be used to scale the performance of these materials. This engineering challenge requires electrical connections between IPMC slabs that prevent short-circuiting between slabs and lubricate the contact between neighboring slabs.

In his studies of IPMCs based on a Nafion117 matrix, Zawodzinski [2000] observed that competition between ion conduction and electro-osmotic migration would limit the minimum effective thickness of IPMC actuators to ~100 μm. He suggests that this is based on matrix topography, solvent, and ion properties. Understanding the required properties of IPMC matrix materials will assist in the development of replacements for Nafion117.

6.8 Acknowledgments

We wish to thank Drs. Steve Wax (DARPA), Len Buckley (NRL), Carlos Sanday (NRL), and Randy Sands for their continued encouragement and many stimulating discussions while the original version of this chapter was being prepared. We thank Prof. Mohsen Shahinpoor and Dr. K. J. Kim for providing the Nafion-based IPMC materials and many informative discussions, and Dr. Kinji Asaka for providing the Flemion-based IPMC materials; also Jon Isaacs (who designed the mini-load frame) and David Lischer for assistance with mini-load frame testing, Jeff McGee for helpful discussions, and Nicolas Daza and Jean-Charles Duchêne, visiting summer students from the Université de Toulon et du Var. This work has been supported by DARPA grant number MDA972-00-1-0004 to the University of California, San Diego.

6.9 References

Abé, Y., Mochizuki, A., Kawashima, T., Yamashita, S., Asaka, K., and Oguro, K., "Effect on bending behavior of counter cation species in perfluorinated sulfonate membrane-platinum composite," *Polym. Adv. Technol.*, v. 9, no. 8, 1998, pp. 520-526.

Agmon, N., "The Grotthuss Mechanism," *Chem. Phys. Lett.*, v. 244, no. 5-6, 1995, pp. 456-462.

Agmon, N., "Proton solvation and proton mobility," *Israel J. Chem.*, v. 39, no. 3-4, 1999, pp. 493-502.

Asaka, K., Oguro, K., Nishimura, Y., Mizuhata, M., and Takenaka, H. "Bending of polyelectrolyte membrane-platinum composites by electric stimuli. Part 1. Response characteristics to various waveforms," *Polymer J.*, v. 27, no. 4, 1995, pp. 436-440.

Asaka, K., and Oguro, K. "Bending of polyelectrolyte membrane platinum composites by electric stimuli, Part II. Response kinetics," *J. Electroanal. Chem.*, v. 480, no. 1-2, 2000, pp. 186-198.

Atkin, R. J., and Fox, N., *An Introduction to the Theory of Elasticity*, London: Longman, 1980.

Bar-Cohen, Y., Xue, T., Shahinpoor, M., Simpson, J. O., and Smith, J., "Low-mass muscle actuators using electroactive polymers (EAP)," Proc. SPIE Vol.3324, pp. 218-223, 1998.

Bar-Cohen, Y., Leary, S., Shahinpoor, M., Harrison, J. O., and Smith, J., "Electro-active polymer (EAP) actuators for planetary applications," *SPIE Conference on Electroactive Polymer Actuators*, Proc. SPIE Vol. 3669, pp. 57-63, 1999a .

Bar-Cohen, Y., Leary, S. P., Shahinpoor, M., Harrison, J. S., and Smith, J., "Flexible low-mass devices and mechanisms actuated by electroactive polymers," Proc. SPIE Vol. 3669, pp. 51-56, 1999b.

Bartrum, B. E. (Dow Chemical Co.), "Process for plating permselective membrane," GB Patent: 1,143,883, 1969.

Belloni, J., Mostafavi, M., Remita, H., Marignier, J. L., and Delcourt, M. O., "Radiation-induced synthesis of mono- and multi-metallic clusters and nanocolloids," *New J. Chem.*, v. 22, no. 11, 1998, pp. 1239-1255.

Bennett, M., and Leo, D.J., "Manufacture and characterization of ionic polymer transducers with non-precious metal electrodes," *Smart Materials and Structures*, vol. 12, no. 3, 2003, pp. 424-436.

Bergman, I. (Minister of Power, London), "Improvements in or relating to membrane electrodes and cells," GB Patent: 1,200,595, 1970.

Blanchard, R. M., and Nuzzo, R. G., "An infrared study of the effects of hydration on cation-loaded nafion thin films," *J. Polym. Sci. B Polym. Phys.*, v. 38, no. 11, 2000, pp. 1512-1520.

Bockris, J. O'M., and Reddy, A. K. N., *Modern Electrochemistry*, v. 2, 1977.

Bockris, J. O'M., and Reddy, A. K. N., *Modern Electrochemistry 1: Ionics*, v. 1, New York: Plenum Press, 1998.

Bonner, O. D., "Study of methanesulfonates and trifluoromethanesulfonates. Evidence for hydrogen bonding to the trifluoro group," *J. Am. Chem. Soc.*, v. 103, no. 12, 1981, p. 3262-3265.

Caldwell, D. G., "Pseudomuscular actuator for use in dextrous manipulation," *Med. Biol. Eng. Comp.*, v. 28, no. 6, 1990, pp. 595.

Caldwell, D. G., and Tsagarakis, N., "'Soft' grasping using a dextrous hand," *Ind. Robot*, v. 27, no. 3, 2000, pp. 194-199.

Chen, Y.-L., and Chou, T.-C., "Metals and alloys bonded on solid polymer electrolyte for electrochemical reduction of pure benzaldehyde without liquid supporting electrolyte," *J. Electroanal. Chem.*, v. 360, no. 1-2, 1993, p. 247-259.

Cwirko, E. H., and Carbonell, R. G., "Ionic equilibria in ion-exchange membranes: a comparison of pore model predictions with experimental results," *J. Membr. Sci.*, v. 67, no. 2-3, 1992, p. 211-226.

Datye, v. K., Taylor, P. L., and Hopfinger, A. J., "Simple model for clustering and ionic transport in ionomer membranes," *Macromolecules*, v. 17, 1984, pp. 1704-1708.

Datye, v. K., and Taylor, P. L., "Electrostatic contributions to the free energy of clustering of an ionomer," *Macromolecules*, v. 18, 1985, pp. 1479-1482.

de Gennes, P. G., Okumura, K., Shahinpoor, M., and Kim, K. J., "Mechanoelectric effects in ionic gels," *Europhys. Lett.*, v. 50, no. 4, 2000,p p. 513-518.

DeWulf, D. W., and Bard, A. J., "Application of Nafion/platinum electrodes (solid polymer electrolyte structures) to voltammetric investigations of highly resistive solutions," *J. Electrochem. Soc.*, v. 135, no. 8, 1988, pp. 1977-1985.

Dube, J. R. (United Technologies Corporation, USA), "Formation of electrode on anion exchange membrane," US Patent: 5,853,798, 1998.

Eisenberg, A., "Clustering of ions in organic polymers, a theoretical approach," *Macromolecules*, v. 3, 1970, pp. 147-154.

Eisenberg, A., and Kim, J.-S., "Ionomers (Overview)" in *Polymeric Materials Encyclopedia* Salamone, J. C., (Ed.) pp. 3435-3454, CRC Press, Boca Raton, FL, 1996.

Fernandez, R. E., "Perfluorinated Ionomers" in *Polymer Data Handbook*, Mark, J. E., (Ed.) p. 233-238, Oxford University Press, New York, 1999.

Feynman, R. P., *Surely You're Joking, Mr. Feynman!*, First Ed., New York: W.W. Norton, 1985.

Forsman, W. A., "Effect of segment-segment association on chain dimensions," *Macromolecules*, v. 15, 1982, pp. 1032-1040.

Forsman, W. A., "Statistical mechanics of ion-pair association in ionomers," *Proceedings of the NATO Advanced Workshop on Structure and Properties of Ionomers*, 1986, pp. 39-50.

Fujita, Y., and Muto, T. (Japan Storage Battery Co., Ltd., Japan), "Manufacture of ion exchange resin membrane-electrode connections," JP Patent: 61,295,387, 1986.

Fujiwara, N., Asaka, K., Nishimura, Y., Oguro, K., and Torikai, E., "Preparation of gold-solid polymer electrolyte composites as electric stimuli-responsive materials," *Chem. Mater.*, v. 12, no. 6, 2000, pp. 1750-1754.

Gebel, G., Aldebert, P., and Pineri, M., "Swelling study of perfluorosulfonated ionomer membranes," *Polymer*, v. 34, no. 2, 1993, pp. 333-339.

Gejji, S. P., Suresh, C. H., Bartolotti, L. J., and Gadre, S. R., "Electrostatic potential as a harbinger of cation coordination: CF3SO3- ion as a model example," *J. Phys. Chem. A*, v. 101, 1997, p. 5678-5686.

Gierke, T. D., Munn, C. E., and Walmsley, P. N., "The morphology in Nafion perfluorinated membrane products, as determined by wide- and small-angle X-ray studies," *J. Polym. Sci., Polym. Phys. Ed.*, v. 19, 1981, pp. 1687-1704.

Heitner-Wirguin, C., "Recent advances in perfluorinated ionomer membranes - structure, properties and applications," *J. Membr. Sci.*, v. 120, no. 1, 1996, pp. 1-33.

Hitachi, "Formation of an electrode film on an ion-exchanging membrane" (Hitachi Shipbuilding and Engineering Co., Ltd., Japan), JP Patent: 58,185,790, 1983.

Homma, M., and Nakano, Y., "Development of electro-driven polymer gel/platinum composite membranes," *Kagaku Kogaku Ronbunshu*, v. 25, no. 6, 1999, pp. 1010-1014.

Hsu, W. Y., and Gierke, T. D., "Elastic theory for ionic clustering in perfluorinated ionomers," *Macromolecules*, v. 13, 1982, pp. 198-200.

Iyer, S. T., Nandan, D., and Iyer, R. M., "Thermodynamic equilibrium constants of alkali metal ion-hydrogen ion exchanges and related swelling free energies in perfluorosulfonate ionomer membrane (Nafion-117) in aqueous medium," *Indian J. Chem., Sect. A: Inorg., Bio-inorg., Phys., Theor. Anal. Chem.*, v. 31A, no. 6, 1992, pp. 317-322.

James, P. J., Elliott, J. A., McMaster, T. J., Newton, J. M., Elliott, A. M. S., Hanna, S., and Miles, M. J., "Hydration of Nafion (R) studied by AFM and X-ray scattering," *J. Mater. Sci.*, v. 35, no. 20, 2000, pp. 5111-5119.

Kordesch, K. v., and Simader, G. R., "Environmental impact of fuel cell technology," *Chem. Re v.*, v. 95, no. 1, 1995, pp. 191-207.

Lakshminarayanaiah, N., *Transport Phenomena in Membranes*, New York: Academic Press, 1969.

Lauer, A., Alley Theater, Houston, TX, personal communication.

Levine, C. A., and Prevost, A. L. (Dow Chemical Co.), "Metal plating permselective membranes," FR Patent: 1,536,414, 1968.

Li, J. Y., and Nemat-Nasser, S., "Micromechanical analysis of ionic clustering in Nafion perfluorinated membrane," *Mechanics of Materials*, v. 32, no. 5, 2000, pp. 303-314.

Liu, R., Her, W. H., and Fedkiw, P. S., "*In situ* electrode formation on a Nafion membrane by chemical platinization," *J. Electrochem. Soc.*, v. 139, no. 1, 1992, pp. 15-23.

Love, A. E. H., A Treatise on the Mathematical Theory of Elasticity, New York: Dover, 1944.

Ludvigsson, M., Lindgren, J., and Tegenfeldt, J., "FTIR study of water in cast Nafion films," *Electrochim. Acta*, v. 45, no. 14, 2000, pp. 2267.

McCallum, C., and Pletcher, D., "Reduction of oxygen at a metallized membrane electrode," *Electrochim. Acta*, v. 20, no. 11, 1975, pp. 811-814.

McGee, J., "Mechano-electrochemical response of ionic polymer-metal composites, " Ph.D Thesis Dissertation, UC San Diego, 2002.

Millet, P., Pineri, M., and Durand, R., "New solid polymer electrolyte composites for water electrolysis," *J. Appl. Electrochem.*, v. 19, no. 2, 1989, pp. 162-166.

Millet, P., Durand, R., and Pineri, M., "Preparation of new solid polymer electrolyte composites for water electrolysis," *Int. J. Hydrogen Energy*, v. 15, no. 4, 1990, pp. 245-253.

Millet, P., Durand, R., Dartyge, E., Tourillon, G., and Fontaine, A., "Study of the precipitation of metallic platinum into ionomer membranes by time-resolved dispersive x-ray spectroscopy," *AIP Conf. Proc.*, 1992, v. 258, pp. 531-538.

Millet, P., Durand, R., Dartyge, E., Tourillon, G., and Fontaine, A., "Precipitation of metallic platinum into Nafion ionomer membranes. I. Experimental results," *J. Electrochem. Soc.*, v. 140, no. 5, 1993, pp. 1373-1380.

Millet, P., Andolfatto, F., and Durand, R., "Preparation of solid polymer electrolyte composites: investigation of the ion exchange process," *J. Appl. Electrochem.*, v. 25, no. 3, 1995, pp. 227-232.

Millet, P., "Noble metal-membrane composites for electrochemical applications," *J. Chem. Ed.*, v. 76, no. 1, 1999, pp. 47-49.

Miyoshi, H., Yamagami, M., and Kataoka, T., "Characteristic coefficients of Nafion membranes," *Chem. Express*, v. 5, no. 10, 1990, pp. 717-720.

Modern Plastics, "Metalizing plastic surfaces," v. 16, Sept., 1938, pp. 30.

Mojarrad, M., and Shahinpoor, M., "Ion exchange membrane-platinum composites as electrically controllable artificial muscles," *Third International Conference on Intelligent Materials*, SPIE Proc. Vol. 2779, 1996, pp. 1012-1017.

Mojarrad, M., and Shahinpoor, M. "Ion-exchange-metal composite artificial muscle actuator load characterization and modeling," SPIE Proc. Vol. 3040, 1997, pp. 294-301.

Nandakumar, P., Vijayan, C., Murti, Y.v.G.S., Dhanalakshmi, K., and Sundararajan, G., "Proton exchange mechanism of synthesizing CdS quantum dots in Nafion," *Indian J. Pure Appl. Phys.*, v. 37, no. 4, 1999, pp. 239-241.

Nemat-Nasser, S., "Micromechanics of Actuation of Ionic Polymer-metal Composites," *J. Appl. Phys*., v. 92, no. 5, 2002, pp. 2899-2915.

Nemat-Nasser, S., and Hori, M., *Micromechanics: Overall Properties of Heterogeneous Materials*, First Ed., Amsterdam: North-Holland, 1993.

Nemat-Nasser, S., and Hori, M., *Micromechanics: Overall Properties of Heterogeneous Materials*, Second Ed., Amsterdam: Elsevier, 1999.

Nemat-Nasser, S., and Li, J. Y. "Electromechanical response of ionic polymer-metal composites," *J. Appl. Phys.*, v. 87, no. 7, 2000, pp. 3321-3331.

Nemat-Nasser, S., and Thomas, C., "Ionomeric polymer-metal composites," *Electroactive Polymer (EAP) Actuators as Artificial Muscles—Reality, Potential, and Challenges*, Yoseph Bar-Cohen, Ed., PM98, SPIE Press, 2001, pp. 139-191.

Nemat-Nasser, S., and Wu, Y., "Comparative Experimental Study of Nafion-and-Flemion-Based Ionic Polymer-metal Composites (IPMC)," *J. Appl. Phys.*, v. 93, no. 9, 2003a, pp. 5255-5267.

Nemat-Nasser, S., and Wu, Y., "Tailoring Actuation of Ionic Polymer-metal Composites Through Cation Combination," *Proceedings of SPIE*, 5051, 2003b, pp. 245-253.

Nemat-Nasser, S., and Zamani, S., "Experimental Study of Nafion-and Flemion-Based Ionic Polymer-Metal Composites (IPMC's) with Ethylene Glycol as Solvent," *Proceedings of SPIE*, 5051, 2003, pp. 233-244.

Oguro, K., Kawami, Y., and Takenaka, H., "An actuator element of polyelectrolyte gel membrane-electrode composite," *Osaka Kogyo Gijutsu Shikensho Kiho*, 43, no. 1, 1992, pp. 21-24.

Oguro, K., Fujiwara, N., Asaka, K., Onishi, K., and Sewa, S., "Polymer electrolyte actuator with gold electrodes," SPIE Proc. Vol. 3669, 1999, pp. 64-71.

Osada, Y., Okuzaki, H., and Hori, H., "A polymer gel with electrically driven motility," *Nature*, v. 355, no. 6357, 1992, pp. 242-244.

Pelrine, R., Kornbluh, R., Pei, Q. B., and Joseph, J., "High-speed electrically actuated elastomers with strain greater than 100%," *Science*, v. 287, no. 5454, 2000, pp. 836-839.

Platzer, O., Amblard, J., Belloni, J., and Marignier, J. L. (Atochem S. A., Fr.), "Ion-exchange fluoropolymers containing metal aggregates and their preparation," EP Patent: 309,337, 1989.

Pomes, R. "Theoretical studies of the grotthuss mechanism in biological proton wires," *Israel J. Chem.*, v. 39, no. 3/4, 1999, pp. 387-395.

Potente, J. M., "Gas-phase electrosynthesis by proton pumping through a metalized Nafion membrane: hydrogen evolution and oxidation, reduction of

ethene, and oxidation of ethane and ethene," Ph.D. Thesis., North Carolina State University, Raleigh, North Carolina, 1988.

Rashid, T., and Shahinpoor, M., "Force optimization of ionic polymeric platinum composite artifical muscles by means of an orthogonal array manufacturing method," *SPIE Conference on Electroactive Polymer Actuators and Devices*, SPIE Proc. Vol. 3669, 1999, pp. 289-298.

Robinson, R. A., and Stokes, R. H., *Electrolyte Solutions*, Second (Revised) Ed., London: Butterworths, 1965.

Roche, E. J., Pineri, M., Duplessix, R., and Levelut, A. M., "Small-angle scattering studies of Nafion membranes," *J. Polym. Sci., Polym. Phys. Ed.*, v. 19, no. 1, 1981, pp. 1-11.

Rollet, A. L., Simonin, J. P., and Turq, P., "Study of self-diffusion of alkali metal cations inside a Nafion membrane," *Phys. Chem. Chem. Phys.*, v. 2, no. 5, 2000, pp. 1029.

Sadeghipour, K., Salomon, R., and Neogi, S., "Development of a novel electrochemically active membrane and 'smart' material based vibration sensor/damper," *Smart Mater. Struct.*, v. 1, no. 2, 1992, p. 172-179.

Sakai, T., Takenaka, H., and Torikai, E. (Agency of Industrial Sciences and Technology, Japan), "Metal-containing ion-exchange membranes for gas separation," JP Patent: 60,135,434, 1985a.

Sakai, T., Takenaka, H., Wakabayashi, N., Kawami, Y., and Torikai, E. "Preparation of Nafion-metal fine particle composite membranes," *Osaka Kogyo Gijutsu Shikensho Kiho*, v. 36, no. 1, 1985b, pp. 10-16.

Salehpoor, K., Shahinpoor, M., and Razani, A. "Role of ion transport in actuation of ionic polymeric-platinum composite (IPMC) artificial muscles," SPIE Proc. Vol. 3330, 1998, pp. 50-58.

Segalman, D. J., Witkowski, W. R., Adolf, D. B., and Shahinpoor, M., "Theory and application of electrically controlled polymeric gels," *Smart Mater. Struct.*, v. 1, no. 1, 1992, pp. 95-100.

Sewa, S., Onishi, K., Asaka, K., Fujiwara, N., and Oguro, K., "Polymer actuator driven by ion current at low voltage, applied to catheter system," *Proc. - IEEE Ann. Int. Workshop Micro Electro Mech. Syst., 11th*, 1998, pp. 148-153.

Shahinpoor, M., "Conceptual design, kinematics and dynamics of swimming robotic structures using active polymer gels," *Act. Mater. Adapt. Struct., Proc. ADPA/AIAA/ASME/SPIE Conf.*, 1992, pp. 91-95.

Shahinpoor, M., "Micro-electro-mechanics of ionic polymeric gels as electrically controllable artificial muscles," *J. Intel. Mat. Syst. Struct.*, v. 6, no. 3, 1995, pp. 307-314.

Shahinpoor, M., "Ionic polymeric gels as artificial muscles for robotic and medical applications," *Iran. J. Sci. Technol.*, v. 20, no. 1, 1996, p. 89-136.

Shahinpoor, M., and Thompson, M. S., "The Venus flytrap as a model for a biomimetic material with built-in sensors and actuations," *Mater. Sci. Eng., C*, v. 2, no. 4, 1995, pp. 229-233.

Shahinpoor, M. "Electro-mechanics of iono-elastic beams as electrically-controllable artificial muscles," *SPIE Conference on Electroactive Polymer Actuators and Devices*, SPIE Proc. Vol. 3669, 1999, pp. 109-121.

Shahinpoor, M., Mojarrad, M., and Salehpoor, K., "Electrically induced large amplitude vibration and resonance characteristics of ionic polymeric membrane-metal composites artificial muscles," SPIE Proc. Vol. 3041, 1997, pp. 829-838.

Shahinpoor, M., Bar-Cohen, Y., Simpson, J. O., and Smith, J., "Ionic polymer-metal composites (IPMCs) as biomimetic sensors, actuators and artificial muscles. A review," *Smart Mater. Struct.*, v. 7, no. 6, 1998, pp. R15-R30.

Shi, M., and Anson, F. C., "Effects of hydration on the resistances and electrochemical responses of Nafion coatings on electrodes," *J. Electroanal. Chem.*, v. 415, 1996, p. 41-46.

Si, Y.-C., Han, Z.-Q., and Chen, Y.-X., "Fabrication of Pt/Nafion membranes," *Huaxue Xuebao*, v. 56, no. 10, 1998, p. 1027-1031.

Sodaye, H. S., Pujari, P. K., Goswami, A., and Manohar, S. B., "Diffusion of Cs^{+} and Zn^{2+} through Nafion-117 ion exchange membrane," *J. Radioanal. Nucl. Chem.*, v. 214, no. 5, 1996, p. 399-409.

Steck, A., and Yeager, H. L., "Water sorption and cation-exchange selectivity of a perfluorosulfonate ion-exchange polymer," *Anal. Chem.*, v. 52, 1980, p. 1215-1218.

Tadokoro, S., Murakami, T., Fuji, S., Kanno, R., Hattori, M., Takamori, T., and Oguro, K., "An elliptic friction drive element using an ICPF actuator," *IEEE Control Systems Magazine*, v. 17, no. 3, 1997, p. 60-68.

Takenaka, H., Torikai, E., Kawami, Y., and Wakabayashi, N., "Solid polymer electrolyte water electrolysis," *Int. J. Hydrogen Energy*, v. 7, no. 5, 1982, p. 397-403.

Takenaka, H., Torikai, E., Kawami, Y., Wakabayashi, N., and Sakai, T., "Solid polymer electrolyte water electrolysis. II. Preparation methods for membrane-electrocatalyst composite," *Denki Kagaku Oyobi Kogyo Butsuri Kagaku*, v. 53, no. 4, 1985, p. 261-265.

Treolar, L. R. G., *Physics of Rubber Elasticity*, Oxford University Press, 1958.

Wax, S. G., and Sands, R. R., "Electroactive polymer actuators and devices," *SPIE Conference on Electroactive Polymer Actuators and Devices*, SPIE Proc. Vol. 3669, 1999, p. 2-10.

Wiechen, A. (Thiele, Heinrich), "Isopor membranes," DE Patent: 1,303,142, 1971.

Xue, T., Trent, J. S., and Osseo-Asare, K., "Characterization of Nafion membranes by transmission electron microscopy," *J. Membr. Sci.*, v. 45, no. 3, 1989, p. 261-271.

Xue, T., Longwell, R. B., and Osseo-Asare, K., "Mass transfer in Nafion membrane systems: effects of ionic size and charge on selectivity," *J. Membr. Sci.*, v. 58, no. 2, 1991, p. 175-189.

Yeager, H. L., Twardoski, Z., and Clark, L., *J. Electrochem. Soc.*, v. 129, 1982, p. 328.

Zana, R., and Yeager, E., "Determination of ionic partial molar volumes from ionic vibration potentials," *J. Phys. Chem.*, v. 70, no. 3, 1966, p. 954-955.

Zawodzinski, T. A., Jr., *220th ACS National Meeting*, Washington, D.C., 2000, v. PMSE - 270.

Zelsmann, H. R., Pineri, M., Thomas, M., and Escoubes, M., "Water self-diffusion coefficient determination in an ion exchange membrane by optical measurement," *J. Appl. Polym. Sci.*, v. 41, 1990, p. 1673-1684.